FACULTY OF MEDICINE AND HEALTH SCIENCES

Evaluating the feasibility to perform vagus nerve stimulation in a rodent model for glioma-related epilepsy

Delphine Dhont

Student number: 01508685

Promotor: Prof. Dr. R. Raedt
Co-Promotor: Prof. Dr. K. Vonck
Mentor: PhD C. Bouckaert

A dissertation submitted to Ghent University in partial fulfilment of the requirements for the degree of Master of Biomedical Sciences

Academic year: 2019 - 2020

GHENT UNIVERSITY

PREFACE

Ever since I was a kid I wanted to be a doctor, but fate decided otherwise. Biomedical Sciences was the best thing that could ever happen to me. Especially in the last two years where I discovered neurological research and sciences. My motivation, curiosity and ambition to become a neurological researcher only grew.

First, I would like to thank my promotor Prof. Dr. Robrecht Raedt to give me the opportunity to investigate the LGG rodent model as a project during my master thesis. This would not have been possible without the guidance of Jeroen Verhoeven. Thank you Jeroen for learning me everything about cell cultures and taking care of my cells in the weekends.

Secondly, I would like to thank my mentor Charlotte Bouckaert. She fulfilled her role as mentor excellently and guided me through two fascinating master years. She gave me a lot of opportunities and trust in doing experiments independently . Thank you Charlotte for believing in me and being such an amazing mentor.

Further, I would like to thank the whole 4BRAIN research group and my colleague students. Thank you for the wonderful ambiance in the lab. In particularly, I would also like to thank Charlotte Germonpré, Marie Goossens, Latoya Stevens and Jana Desloovere for helping me out when Charlotte Bouckaert was not available.

Last but not least, a special thank you for my family, boyfriend and friends to support me and dealing with my stress during the last two years. Without you all it was not possible to have such two amazing master years.

TABLE OF CONTENTS

SUMMARY

Background. 50-90% of low-grade glioma (LGG) patients and 20-60% of high-grade glioma patients have epileptic seizures. Additional treatment with anti-epileptic drugs can have severe side effects. **1.** Immune cells of the tumour micro-environment express α7nAchR. Thereby, vagus nerve stimulation (VNS) could influence glioma progression via the cholinergic anti-inflammatory pathway. Feasibility to perform VNS in a glioblastoma-related epilepsy rat model was investigated. **2.** A potential LGG model was investigated since LGG patients present more often with seizures.

Methods. 1. MaleF344/IcoCrl rats were implanted with a VNS electrode and EEG recording electrodes, and F98 glioblastoma cells were inoculated. From day 7 to 14 post-inoculation brain activity was monitored. At day 10, VNS stimulation (30Hz, biphasic pulses (250µs/phase), 0.5sec ON/29.5sec OFF) was initiated in half of the animals at an intensity of 250µA and increased daily in steps of 250µA until day 13. **2.** Grade I and II glioma cells were injected in three non-immunocompromised rats and one RNu rat and immunocytochemistry was performed on both cell lines.

Results. **1.** Stimulated animals had tumour volumes of 11.66 and 8.18mm^3 and one non-stimulated animal had a tumour volume of 16.96mm^3. Only one out of six animals had seizures. **2.** Both cell lines stained negative for glial fibrillar acidic protein and no tumour growth was obtained.

Discussion. 1. So far our data is still inconclusive regarding the effect of VNS on glioma progression and seizures. Further experiments with longer EEG monitoring are needed. **2.** Further studies should first investigate the characteristics of long cultured cells.

INFLUENCE OF SARS-COV2

1. VNS experiment

Normally, the blood samples that were taken from the animals at several time points in the study (mentioned in material and methods) would have been analysed for specific markers. This was not possible due to the Sars-CoV-2 outbreak. The results obtained from the analyses of the blood samples would have helped to estimate the effect of tumour growth, VNS and seizures on certain inflammatory parameters. Secondly, more VNS studies would have been conducted if there was no Sars-Cov-2 outbreak. Thereby, we possibly would have had significant results or a better idea about the effects of VNS on glioma progression and glioma-related seizures. Additionally, we could have adjusted our studies, for example longer EEG monitoring. Without these additional studies it was not possible to make a significant conclusion about the effects of VNS on glioma progression and glioma-related epilepsy in this master thesis.

The Sars-CoV-2 outbreak could also have influenced the quality of slicing as the slices of all animals were made in one day. This was needed to perform the cresyl violet staining of all animals in one day and thereby minimize the time in the lab.

2. Low-grade glioma model

For the *in vitro* experiments and the immunocytochemistry staining, the F98 cells could not be stained for vimentin. This would have given additional information in the comparison between the LGG cell lines and the F98 cell line and could have concluded the low-grade characteristics of the Res186 and Res259 cells.

For the *in vivo* experiments it was not possible to inject the RNu rat with 100 000 Res259 cells in 5µl PBS in the left and right entorhinal cortex. This would have given a better estimation about the possible tumour growth of the Res259 cells in a T cell deficient rat and could have been one step closer towards an LGG rodent model. Furthermore, an *ex vivo* MRI would have been carried out in the perfused RNu rat. The animal was perfused from the moment the government measures were in place and no further experiments could be done. The idea was to make an *ex vivo* scan before the deadline of this master thesis, to exclude tumour growth with certainty. It was not possible to perform an *ex vivo* MRI in time due to ongoing Sars-CoV-2 outbreak and government measures.

INTRODUCTION

1. Glioma-related epilepsy

1.1 Glioma tumours

Gliomas are the most prevalent primary intracranial tumours, representing 81% of all malignant brain tumours in human[1]. The overall age adjusted incidence of gliomas is 4.67-5.73 per 100 000 persons worldwide and these tumours are more prevalent in males[1,2]. Gliomas are derived from supportive non-neuronal glial cells within the central nervous system (CNS). Non-neuronal glial cells include different cell types, each fulfilling their own function within the CNS. Firstly, astrocytes are responsible for neuronal-glial communication, synaptic signalling, maintenance of the blood-brain barrier (BBB) and have a trophic, metabolic and structural support for neurons[3]. Secondly, oligodendrocytes play a key role in the production of the myelin sheath that insulates axons and is responsible for the fast information transduction of neurons[4]. Thirdly, ependymal cells are involved in the production of cerebrospinal fluid (CSF) and are an essential component of the blood-brain and brain-CSF barrier[5]. Finally, microglia function as the first form of active immune defence within the CNS[6].

Furthermore, gliomas are classified according to their presumed non-neuronal glial cell of origin ("astrocytoma", "oligodendroglioma", "ependymoma" and "glioblastoma") and according to their grade (low-grade vs. high-grade gliomas), which will determine their pathology and progression[7]. Low-grade gliomas (LGGs), World Health Organisation (WHO) grade I and II, are not anaplastic meaning they will not lose their cellular differentiation[8]. Grade I gliomas occur mainly in children and are together with grade II gliomas characterised by slow growth and progression but often possess a malignant transformation over time[2]. The prognosis and overall survival of LGGs is partly defined by mutations in the *isocitrate dehydrogenase* (*IDH)* genes *1* and *2* which are recognised as an early marker for glioma genesis. Patients suffering from LGGs containing *IDH* gene mutations have an improved prognosis compared to patients without *IDH* mutations[2]. High-grade gliomas (HGGs), WHO grade III and IV, are anaplastic meaning they will lose their cellular differentiation during disease progression[9]. Therefore, HGGs have a worse prognosis compared to LGGs and grade IV glioma or glioblastoma (GB) possesses the worst prognosis and survival[2]. Furthermore, epigenetic silencing of the *methyl-guanine methyl transferase* (*MGMT*) gene promotor due to methylation is a crucial prognostic factor in HGGs and LGGs for overall and progression free survival[2,10]. *Methyl-guanine methyl transferase* is an enzyme responsible for DNA repair and patients who are diagnosed with a methylated *MGMT* gene promotor will therefore have a better response to chemotherapy than patients with an unmethylated *MGMT* gene promoter. Additionally, the prognosis of LGG and especially these with oligodendroglial components is strongly influenced by the presence of the loss of heterozygosity (LOH) or co-deletion of 1p/19q[2,11]. The co-deletion or LOH of 1p/19q is established by the chromosomal translocation between chromosome 1 and 19[2]. Patients which are diagnosed with LGG or oligodendrogliomas containing this co-deletion or LOH have a prolonged survival without treatment and a higher sensitivity for radio- and chemotherapy[2,11]. Finally, the expected survival of glioma patients based on grade and origin is illustrated in Figure 1.

Grade and cell type	Median survival
Grade II	
Astrocytoma	7–10 years
Oligodendroglioma[a]	>10–15 years
Grade III	
Anaplastic astrocytoma	3.5 years
Anaplastic oligodendroglioma[a]	>10 years
Grade IV	
Glioblastoma	15 months, 2-year survival 27%
MGMT	
Methylated	23 months, 2-year survival: 49%
Unmethylated	13 months, 2-year survival: 12%

[a]With LOH 1p/19q. MGMT, methyl-guanine methyl transferase

Figure 1. Expected survival of gliomas based on grade and origin and some molecular markers. Figure from Stupp et al., 2014.

1.2 Epileptogenesis of gliomas

The most common symptom in patients with gliomas is the manifestation of epileptic seizures[12]. Therefore, gliomas are responsible for the phenomenon of glioma-related epilepsy according to the International League Against Epilepsy (ILAE)[13]. An epileptic seizure is defined by the ILAE as a transient occurrence of signs and/or symptoms due to abnormal or synchronous neuronal activity in the brain. Epilepsy can be defined as a chronic disease characterised by recurrent seizures[13]. Patients with LGGs are more vulnerable to epileptic seizures (50-90%) than patients with HGGs (20-60%)[8]. The lower vulnerability to seizures in HGGs is probably due to their characteristics of rapid and invasive tumour growth which might preclude epileptogenesis and some patients will not survive long enough to develop these glioma-related seizures[14].

The mechanism and origin of glioma-related epilepsy is not clear yet. Two epileptogenic approaches are considered for the moment.

1.2.1 Tumourocentric hypothesis

Gliomas are space-occupying brain tumours and can therefore contribute to epileptic activity[15]. The mechanical effects of mass and oedema are responsible for microcirculation impairments by local hypoperfusion which is responsible for ischemic changes in the surrounding neocortex. LGGs, characterised by slow growth and invasion of the surrounding brain tissue, are responsible for isolation and deafferentation of the cortico-subcortical local and distant networks, resulting in epileptogenesis[15]. Conversely, HGGs are characterised by rapid and invasive tumour growth and neoangiogenesis will occur in these gliomas, meaning new blood vessels will be formed. This process will be responsible for acute tissue damage such as haemorrhage and necrosis. Furthermore, the BBB of these newly formed blood vessels will become permeable to pro-epileptogenic molecules and immune cells. In the end, these processes might contribute to the epileptogenicity of gliomas.

1.2.2 Epileptocentric hypothesis

The epileptocentric hypothesis is based on dysregulation of the equilibrium between excitatory and inhibitory signals in the brain[15]. This hypothesis can be clarified by two different assumptions namely the glutamatergic mechanisms or the GABAergic mechanisms.

1.2.2.1 Glutamatergic mechanisms

Firstly, gliomas express an upregulated amount of the Xc- cystine glutamate transporter, a sodium and chloride dependent antiporter of the anionic forms of cystine and glutamate (Glu)[16]. The mechanism of action of this transporter is illustrated in Figure 2[16]. Although this transporter can exchange the molecules in both directions, the transport will only take place in one direction for each molecule. This one-way transport is due to the low intracellular concentration of cystine, caused by the immediate metabolization into cysteine after being transported into the neuron and the low extracellular concentration of Glu (2-9 µM) (which is) necessary for optimal neurotransmission. Therefore, cystine will be transported intracellularly for a 1:1 counter transport of glutamate extracellularly. Once cystine is transported into the cell it will be immediately converted to cysteine, which is further used for the synthesis of antioxidant glutathione (GSH)[15]. GSH is the most important antioxidant within the brain. GSH will reduce high levels of free radicals like reactive-oxygen species (ROS), which are produced by oxidative phosphorylation in the mitochondria during production of adenosine triphosphate

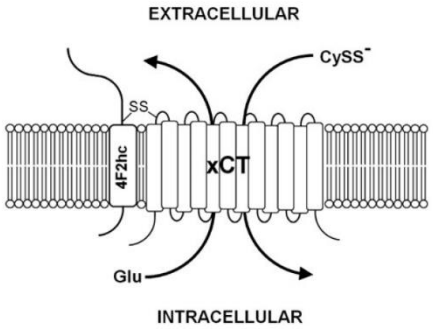

Figure 2. System Xc- is composed of the 4F2 heavy chain and the xCT light chain, which are linked by a disulfide bond. System Xc- imports cystine (CySS-) in exchange for glutamate (Glu). Figure from Lewerenz et al., 2013.

(ATP)[17]. This oxidative stress is responsible for oxidative modification of lipids, proteins and DNA, resulting in cell death[16]. High concentrations of extracellular Glu can inhibit this Xc- transporter resulting in the inhibition of the GSH synthesis[18]. Thereby excessive Glu concentrations are responsible for oxidative glutamate toxicity. The excessive expression of this Xc- transporter will protect the glioma cells against their excessive Glu release and the related oxidative glutamate toxicity. Secondly, some gliomas lack the excitatory amino acid transporters (EAATs)[15]. These EAATs fulfil the key role in the rapid re-uptake of released Glu in the synaptic cleft. There exist five different types of EAATs. Glioblastomas and astrocytomas lack EAAT1 and EAAT2 which are expressed by astrocytes for the immediate re-uptake of Glu[16]. The mechanism of action of these transporters is based on the co-transport of Na^+ ions and protons for each molecule of Glu that is transported into the cell and the counter transport of K^+ ion extracellularly. Therefore, the EAATs are capable of transporting Glu against its high concentration gradient. Taken together, gliomas can be responsible for the high extracellular concentration of Glu due to the lack of EAATs for Glu re-uptake and the overexpression of Xc- transporters. Thereby more excitatory signals will appear in the environment of a glioma resulting in an imbalance between the inhibitory and excitatory signals in the brain. Eventually, this phenomenon will give rise to epileptogenicity.

1.2.2.2 GABAergic mechanisms

The imbalance between inhibitory and excitatory signals is observed in multiple epileptic disorders[15]. Gliomas are characterised by the excessive expression of gamma-aminobutyric acid (GABA) receptors, which contribute to the fast volume reduction of the cells. This process is required for proliferation and migration of gliomas. Furthermore, reduced GABAergic inhibitory pathways are observed in the peritumoral cortex[15]. This reflects a reduction in inhibitory GABA interneurons and inhibitory synapses on pyramidal cells around the tumour.

GABAa receptors are ion channels responsible for hyperpolarisation of neurons by influx of chloride ions after binding of GABA on the receptor[19]. The excessive expression of GABAa receptors in glioma cells is responsible for crucial changes in the chloride homeostasis and partly engaged in the increased intracellular chloride concentration needed for fast volume reduction[15]. Increased intracellular chloride concentrations will create an outwardly driven force for the movement of chloride followed by water[20]. When the outward flow of chloride is inhibited in proliferating cells, there will be no condensation of chromatin into chromosomes. This process is needed for cell division. Therefore, the fast volume reduction due to the high intracellular chloride concentrations and the high chloride conductance of glioma cells will provide a signal to the glioma cell to continue cell division. This way, stimulation of the GABAa receptor can enhance glioma progression. Furthermore, the $Na^+/K^+/2Cl^-$ co-transporter 1 (NKCC1) is highly expressed in glioma cells and their peritumoral cortex[15]. These NKCC1 transporters are accountable for high intracellular chloride concentrations which are also typically expressed during neuronal development[15,19]. These high intracellular chloride concentrations in the peritumoral neurons will influence the reversal potential of chloride, resulting in the disappearance of the GABAergic inhibitory effect[19]. Additionally, the expression of the potassium-chloride (KCC2) co-transporter is decreased in glioma cells and their peritumoral cortex. This co-transporter is

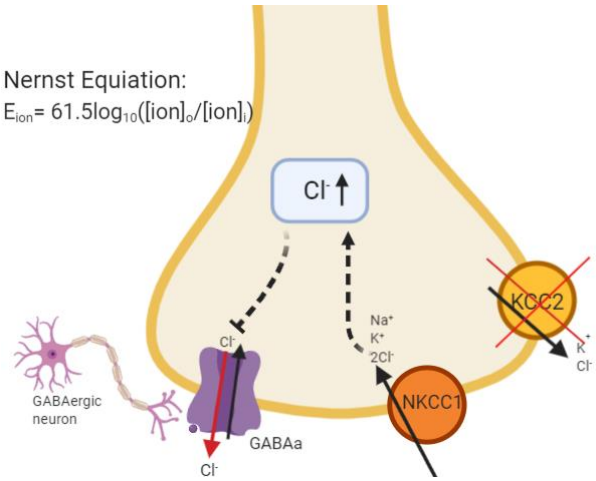

Figure 3. GABAergic role in epileptogenesis by the depolarising effect of GABA. Depolarisation is possible due to high intracellular Cl^- concentration in response to upregulation of NKCC1 co-transporters and downregulation of KCC2 co-transporters. Higher intracellular chloride concentrations will increase the reversal potential of chloride. Image created using BioRender.

in healthy circumstances accountable for low intracellular chloride concentrations and protection against neurotoxicity and overexcitability[15,19]. The overexpression of NKCC1 and decreased expression of KCC2 transporters in glioma cells and peritumoral neurons are mediated by brain-derived neurotrophic factor (BDNF) release of glioma cells or activated microglia[15]. However, stimulation of GABAa receptors in the peritumoral neurons which have increased expression of NKCC1 and decreased expression of KCC2 transporters will result in depolarisation of the cell and will stimulate epileptogenesis[15]. The GABAergic role during epileptogenesis is illustrated in Figure 3.

1.3 Role of inflammation in glioma growth

Inflammation is crucial in cancer development and progression[21]. Even more, the role for inflammation in tumorigenesis is now generally accepted and the inflammatory tumour microenvironment (TME) has become an essential component of all tumours. Tumour associated macrophages (TAMs) are by far the most important immune cells within the TME of GB and are present at all stages of tumour progression[21,22]. TAMs are proven to promote GB growth, invasion and metastasis by the release of tumour necrosis factor α (TNF-α) and interleukin-6 (IL-6)[22,23]. Furthermore, the secreted TNF-α in TME plays a crucial role in cancer progression[21]. In general, two different phenotypes of TAMs can be distinguished namely the M1 and M2 phenotype.

Firstly, the M1 phenotype functions as potent killer of pathogens or tumour cells and is mainly activated after TLR-4 or IFN-γ binding[21,22]. The absence of M1 orientating signals in the TME was already early linked to increased tumour growth *in vitro* and *in vivo* in experimental animal models[23]. But, the associated pathways of M1 TAM phenotype have recently been associated with glioma growth for example by the release of IL-1β[22]. Secondly, the M2 phenotype is generally associated with a pro-tumoral role and activated by IL-4, IL-10 and IL-13 exposure[21,22]. In the TME of GB, the TAMs mostly resemble the M2 phenotype which can promote tumour progression by the release of growth factors, immunosuppressive molecules, chemokines and cytokines[21]. Inhibition of the nuclear factor κB (NF-κB) results in the inversion of the pro-tumoral M2 phenotype into the anti-tumoral M1 phenotype. Thereby the maintenance of the M2 phenotype is suggested to be regulated by NF-κB[21].

1.4 Standard of care for high-grade gliomas

High-grade gliomas such as GB are currently treated multidisciplinary[24]. Multidisciplinary treatment includes the combination of maximal surgical resection of the tumour, radiotherapy (RT) and chemotherapy with temozolomide (TMZ). Firstly, new patients diagnosed with GB will undergo surgery but pre-operative issues such as medical condition, neuropsychological state of patient and the use of corticosteroids or anti-epileptic drugs (AEDs) should be considered. Corticosteroids control cerebral oedema and signs of intracranial hypertension. In this way the administration of corticosteroids will improve brain conditions for surgical resection of the GB[24]. The goal of surgical resection is the realisation of maximal safe resection, obtaining tissue for pathological diagnosis, improve conditions for complementary treatment, delaying clinical worsening and the improvement of quality of life of the patient. Secondly, complementary treatment including TMZ and RT is applied after maximal safe resection of the tumour and followed by a maintenance treatment including six cycles of TMZ. Combined treatment of TMZ and RT after surgical resection has an improved effect on overall survival and progression free survival compared to RT alone[24]. Temozolomide is an oral chemotherapeutic drug which induces DNA methylation and tumour cytotoxicity through blocking the cell cycle. Furthermore, the cytotoxicity of TMZ is apparent by the formation of O6-methylguanine DNA which is repaired by the enzyme MGMT. Additionally, the primary resistance mechanisms to TMZ in GB will be dependent on MGMT activity within the tumour. In the end, when tumours recur, treatment options include supportive care, reoperation, re-irradiation, systemic therapies and combined modality therapy[24].

1.5 Standard of care for low-grade gliomas

Since patients who suffer from LGGs have a longer overall survival, considerations of treatment toxicity as consequence of radio- and chemotherapy have to be taken into account[25]. In patients with LGG, the decision for surgical resection is more complicated than in patients with HGG. Only if a patient shows clear signs due to the mass effect of the tumour or has uncontrolled seizures, surgical resection will be considered. Controversially, many LGGs are discovered by accident during imaging of the brain for other reasons such as headaches and traumas and are therefore asymptomatic. The decision for surgical resection of an asymptomatic LGG is much more complicated[25]. The same conclusion as in surgical resection of HGGs can be made for LGGs. The greater the extent of resection, the lower the chances of recurrence of the tumour and malignant transformation. Therefore, patients with LGGs are recommended to undergo the greatest degree of safe surgical resection. Furthermore, treatment after surgical resection is managed for each patient individually and risk-benefit ratio of RT and chemotherapy is considered. It is crucial that patients undergo long-term surveillance after surgical resection because the tumour can recur. Therefore, patients will undergo further treatment including RT, chemotherapy and/or regular magnetic resonance imaging (MRI) surveillance (Figure 4)[25]. Radiotherapy is not without the risk of short- and long-term adverse effects including fatigue, cognitive decline and memory deficits. In general, combination therapy of RT and adjuvant TMZ chemotherapy also results in an improved overall survival. In the end, the prognosis of patients suffering from LGGs is affected by different factors and varies from two years to decades[25]. Therefore, quality of life and neurocognition of the patients will play a crucial role in treatment decision making.

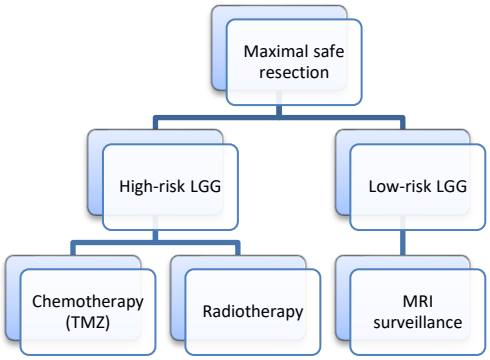

Figure 4. Standard of care for LGG. Patients are divided into two groups, high- and low-risk LGGs, based on clinical features such as age and extent of surgical resection.

1.6 Glioma-related epilepsy

Glioma-related seizures are often resistant to AEDs or tumour resection[2]. The difficulties of a successful treatment in these patients is defined by two factors[26]. Firstly, the number of patients who develop medication-resistant epilepsy is approximately 30-40% of the LGG patients and 15-25% of the GB patients. Seizures within these patients cannot be controlled by administration of AEDs[26,27]. A well-considered reason for the development of medication-resistant epilepsy is the overexpression of the ATP-binding cassette (ABC) transporter family proteins such as P-Glycoprotein (MDR-1), MRP1 and MRP5 in glioma patients[26]. These transporter proteins function as an efflux pump in the endothelial cells of the BBB and will transport lipophilic drugs out of the brain parenchyma into the systemic circulation. Since most of the AEDs administered to glioma patients function as a substrate for these ABC transporter proteins, an insufficient concentration of AEDs remains within the brain parenchyma. However, levetiracetam and valproic acid are no substrates for these proteins and are therefore preferred to treat medication-resistant epilepsy in glioma patients[26].

Secondly, there is a risk for drug-drug interactions during treatment which can result in insufficient control of seizures or tumour activity and drug toxicity in glioma patients[26]. On the one hand, first generation AEDs (phenytoin, carbamazepine, phenobarbital, primidone and their derivates) are known as strong inducers of the hepatic metabolism, namely the cytochrome P450 (CYP) co-enzyme system responsible for the degradation of pharmaceuticals[2,26]. Therefore, administration of these AEDs in glioma patients also receiving other treatments can result in insufficient plasma levels of these medications. Besides this, hepatic degradation of pharmaceuticals is also managed through the UDP-

glucuronosyltransferase (UGT) and the glucuronidation system[26]. Valproic acid is a well-known UGT enzyme inhibitor and administration of this AED can therefore result in an increased, even toxic plasma concentration of pharmaceuticals metabolized by these enzymes. On the other hand, chemotherapeutic agents can be enzyme inducers, for example of the 3A4 co-enzyme, resulting in insufficient plasma concentrations of the administered AEDs, such as carbamazepine, and a higher risk for seizures and developing medication-resistant epilepsy. In conclusion, second and third generation AEDs (such as gabapentin, levetiracetam and topiramate) are preferable in glioma patients because they do not interfere with other administered therapeutics, especially when patients require an intensive medical treatment with several therapeutics[26]. A lot of AEDs can possibly interact with administered chemotherapeutic agents in glioma patients, but not all of these agents are influenced by AEDs, for example TMZ (standard therapy in GB)[2,26]. However, adverse drug reactions can still occur[26]. Temozolomide for example can induce severe thrombopenia and therefore an AED which will lower the blood platelets levels such as valproic acid, is not recommended in these situations[26].

Guidelines for the treatment of glioma-related seizures include that AEDs are only indicated in patients presenting with seizures and after tumour resection the administration of AEDs should be revised and only continued when seizures still occur[2]. Furthermore, antitumoral therapy can also be effective in controlling seizures[26]. Surgical resection of the tumour can result in seizure freedom or control of medication-resistant epilepsy, especially in LGG patients and children. In addition, RT can result in a decreased seizure frequency of 75% for at least 12 months and TMZ can reduce seizure frequency in 50-60% of GB patients.

Besides difficulties in treatment of glioma-related seizures due to drug-drug interactions and development of medication-resistant epilepsy, AEDs in glioma patients also have a negative impact on cognition and quality of life[26]. Glioma patients experience brain damage due to the presence of a tumour, standard of care or previous surgical treatment. However, standard of care and surgical resection of the tumour are nowadays considered as safe. The administration of AEDs can still enhance the subtle noxious effects of these therapies which may result in substantial cognitive damage. In addition, AEDs themselves and the manifestation of seizures have several side-effects on the quality of life of glioma patients[2]. Taken all together, AEDs are often not the best option to treat glioma-related epilepsy and the need for an alternative treatment is growing.

2. Vagus nerve stimulation

2.1 Vagus nerve stimulation for medication-resistant epilepsy

Vagus nerve stimulation (VNS) is a neurophysiological and neuromodulatory treatment developed in the late 1980s and currently broadly used in patients with medication-resistant epilepsy[28,29]. This therapy was initially only approved for partial onset seizures in adults (>12 year) but is extended to several forms of epilepsy and is also administered to children[29]. In these patients, a bipolar spiral electrode is wounded around the left cervical vagal nerve and subcutaneously connected to a pulse generator which delivers electrical pulses and is implanted in the sub-clavicular area (Figure 5)[30]. The right vagus nerve is responsible for the innervation of the sinoatrial node and closely associated with the cardiac atrial function. Therefore the left vagus nerve is chosen to minimize the vagal effects on the heart[29]. The telemetric programming unit makes it possible to programme and adjust the stimulation parameters including output current, pulse width, frequency and duty cycle[30]. VNS requires an invasive surgical procedure, but the discomfort of the surgery and acute/chronic side effects are mild, mainly transient and will

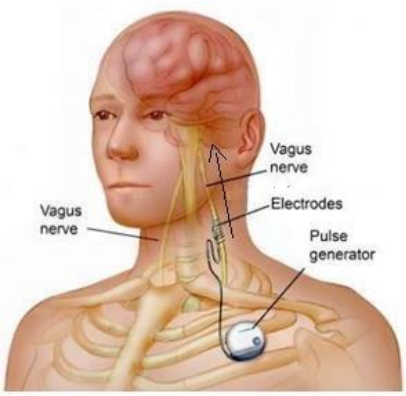

Figure 5. Implanted VNS electrode in a patient. Figure from G. Bedi, 2014.

disappear a few weeks after surgery. Hoarseness, a tingling sensation in the throat and coughing are the most prevalent side effects. The efficacy of VNS within one year is estimated around 50% reduction in seizure frequency in at least 1/3 of the patients with medication-resistant epilepsy[29,30]. But more responders are observed over time, up to 60-70% after five year[29]. Furthermore, long-term VNS in patients showed an improved quality of life in several clinical studies.

The precise mechanism of action of VNS and how it suppresses epileptic seizures is still not completely understood[29]. The vagus nerve is the 10th cranial nerve consisting of 80% afferent fibres and 20% efferent fibres[26,28]. The afferent fibres originate in the nodose ganglion and primary project towards the nucleus tractus solitarii (NTS) (Figure 6) which projects towards several regions of the forebrain, brainstem and important structures in epileptogenesis such as the amygdala and thalamus[28]. Besides these projections, the NTS has also direct connections towards the raphe nuclei, major source of serotonin, and indirect connections towards the locus coeruleus (LC) and A5 nuclei (a group of noradrenergic neurons in the brainstem), both noradrenergic sources. In literature, several research groups tried to identify potential anatomic brain structures which mediate the antiseizure effect of VNS in animals[28]. Increased activity of the amygdala, the thalamus, the LC and the A5 nuclei was observed after VNS in animals. VNS was responsible for the bilateral activation of all these brain structures, confirming the bilateral anticonvulsant effect despite the unilateral stimulation. The amygdala is a highly epileptogenic region that plays a crucial role in the generalization of seizures and the thalamus is also implicated in seizure regulation. Furthermore, the crucial role of the LC was demonstrated by the bilateral dissection of the LC which was accompanied by loss of the seizure supressing effect of VNS by minimizing the norepinephrine release in the brain. In patients, VNS is also able to suppress seizures in the 'off' mode suggesting an anti-epileptic effect. Even more, some literature suggests that seizures might be predicted early enough to trigger stimulation of the vagus nerve[28]. Furthermore, the anti-epileptic effect can also partly be described by the observed increase of GABA in the CSF in patients receiving VNS[28,29].

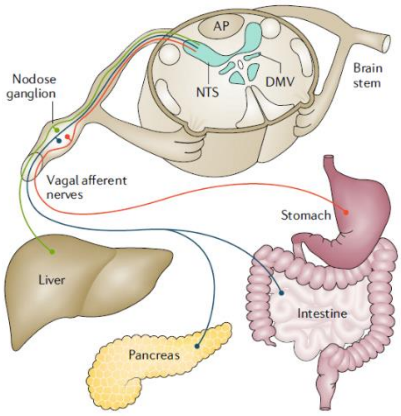

Figure 6. At the subdiaphragmatic level, vagal afferent neurons innervate the stomach, intestines, liver and pancreas and relay. Figure from Waise et al., 2018.

2.2 Anti-inflammatory effect of vagus nerve stimulation

The neuronal response mechanism of the anti-inflammatory pathway relies on the activation of the sensory afferent vagus nerve fibres which provide a signal to the brain that inflammation is occuring[31]. Thereby, the vagal afferent neuronal pathway is suggested to play a dominant role in mild to moderate peripheral inflammatory responses. Via the efferent vagus nerve fibres the anti-inflammatory pathway will be activated. The efferent vagus nerve neurons include the NTS which connects towards hypothalamic nuclei including the paraventricular nucleus (PVN). This PVN releases the corticotrophin releasing hormone (CRP) which in his turn activates the hypothalamic-pituitary-adrenal (HPA) axis by releasing the adrenocorticotropic hormone (ACTH) as illustrated in Figure 7. The latter forms the connection towards the humoral anti-inflammatory pathway and thereby the ascending link between the NTS and the PVN modulates the neurohormonal anti-inflammatory response[31]. Besides this, the NTS possesses also indirect connections towards the LC via the rostral ventrolateral medulla (RVM) (Figure 7). The LC innervates in his turn higher brain structures such as the hypothalamus and the PVN in a noradrenergic manner (Figure 7). In addition, the PVN has also descending projections towards the NTS and the RVM. In conclusion, all these ascending and descending connections of the PVN result in an immunomodulatory role for neurons on the HPA axis[31].

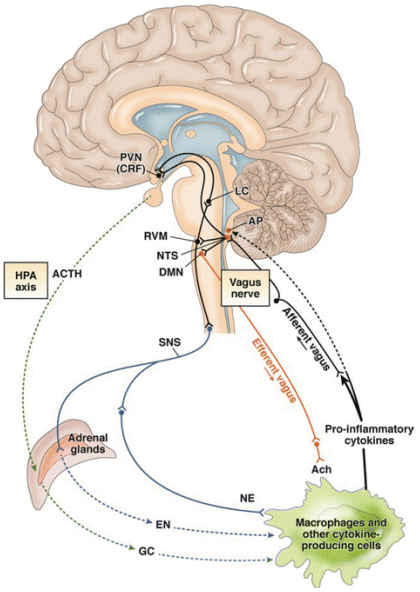

Figure 7. Neuronal response mechanism of the anti-inflammatory pathway in response to systemic inflammation. NTS, nucleus tractus solitarii; DMN, dorsal motor nucleus of the vagus; PVN, paraventricular nucleus; RVM, rostral ventrolateral medulla; LC, locus coeruleus; *SNS, sympathetic nervous system; ACTH, adrenocorticotropin hormone; GC, glucocorticoids; EN, epinephrine; NE, norepinephrine; ACh, acetylcholine. Figure from Bonaz and Bernstein, 2013.*

The cholinergic anti-inflammatory pathway is suggested as the key player in the anti-inflammatory effect of VNS[31]. Acetylcholine (Ach) is a crucial neurotransmitter (NT) and neuromodulator within the brain. This NT mediates the synaptic signalling in the ganglionic synapses of the sympathetic and parasympathetic neurons and is the main NT of vagal efferent neurons. Acetylcholine can bind on two different types of receptors, the muscarine receptor (metabotropic) and the nicotinic receptor (ionotropic)[31]. The RNA of these receptors has been detected in a mixed population of lymphocytes and other (non-)immune cytokine producing cells. Furthermore, the α seven subunit of the nicotinic receptor (α7nAchR) is found on macrophages. Binding of Ach on the α7nAchR of macrophages will result in a decreased production TNF-α and an effective suppression of IL-1β, IL-6 and IL-18 by post transcriptional mechanisms[31]. The direct role of the vagus nerve in suppression of TNF-α levels was suggested via vagotomy in rats resulting in increased TNF-α levels in response to an intravenous injection of endotoxins. VNS resulted in significantly attenuated TNF-α levels after endotoxin

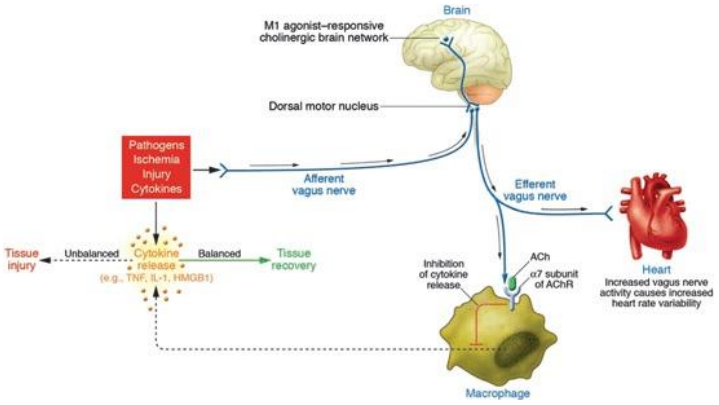

Figure 8. The cholinergic anti-inflammatory pathway. Pro-inflammatory cytokines activate the afferent vagus nerve fibres which (in)directly stimulate the NTS. The NTS will activate the vagal afferents in the dorsal motor nucleus and the vagal efferent fibres will activate the cholinergic anti-inflammatory effect. Figure from Garzoni et al., 2013.

introduction. TNF-α amplifies inflammation by the release of IL-1, HMGB1, nitric oxide, and reactive oxygen species. Based on these findings the vagus nerve has a crucial role in maintaining immunological homeostasis. In the end, the involvement of the efferent vagus nerve neurons in neuromodulation is supported by the protective role of the cholinergic anti-inflammatory pathway which is activated by the vagus nerve[31]. The activation of the cholinergic anti-inflammatory pathway by the vagus nerve is illustrated in Figure 8. Additionally, the NTS may integrate the cholinergic anti-inflammatory pathway into other central immunomodulatory responses[31]. This way, VNS may present a novel approach to inhibit the release of pro-inflammatory cytokines such as TNF-α, IL-1β, IL-6 and IL-18, and thereby protects the patient against pathological inflammation.

Furthermore, VNS also resulted in decreased levels of IL-1β and TNF-α and increased levels of IL-10 in the brain tissue and serum, after a traumatic brain injury in rabbits[32]. Altered levels in brain tissue suggest that the anti-inflammatory effect of VNS is also valid within the brain itself. Additionally, electrical stimulation of the efferent vagal nerves in a haemorrhage shock model resulted in significantly decreased NF-κB activation[21].

3. Glioblastoma-related epilepsy rodent model

Glioblastoma is a grade IV glioma and is responsible for the development of seizures in 30-60% of the patients[26]. Therefore, a GB-related epilepsy rodent model is desired to investigate possible therapies against tumour growth and GB-associated seizures. There exist a lot of GB rodent models but almost studies did not investigate related seizures or these models are not reproducible[33].

Recently, the 4BRAIN research group successfully established a GB-related epilepsy rat model[33]. Therefore, 20 000 F98 cells were inoculated in the right entorhinal cortex, susceptible for the development of epileptic activity, of male F344/IcoCrl rats. The F98 cell line is a N-ethyl-N-nitrosourea-induced glioma cell line and isolated out of a female Fischer 344 rat on the 20st fetal day and has a doublings time *in vitro* of approximately 13 hours *(ExPASy, Bioinformatics Resource Portal, cellosaurus*)[34]. In all animals GB growth was confirmed using T2 weighted MRI. In order to detect seizures in these animals, electrodes to record electroencephalography (EEG) were implanted after confirmation of tumour growth and video-EEG was continuously monitored until euthanasia. During a common 8-day period (day 13 to day 20 post-inoculation) all GB animals had seizures with a mean of 15 ± 11 seizures per animal and no seizures were detected in control animals. All animals were euthanized 21 days post-inoculation based on humane endpoints. Furthermore, immunohistochemical staining for glial filament acidic protein (GFAP) and vimentin, both astrocytic markers, confirmed the astrocytic origin of the tumour.

4. VNS as treatment for glioma-related epilepsy? A hypothesis

This master thesis partly investigated the feasibility to perform VNS as a therapy for glioma and related seizures. Treatment with VNS could provide serious advantages in glioma patients targeting both epileptic seizures, resulting from gliomas, and glioma progression. This hypothesis is based on two fundamental working mechanisms of VNS.

Firstly, VNS could influence the TME by the activation of the cholinergic anti-inflammatory pathway. Via this pathway VNS will be responsible for the suppression of TNF-α, IL-6, IL-1β and NF-κB[31]. Since research illustrated that the TME mainly consists out of innate and adaptive immune cells and most of them express the α7nAchR, VNS might target the TME via his cholinergic anti-inflammatory pathway[21]. To begin, TNF-α and IL-6 are crucial cytokines for the promotion of glioma growth and invasion[22,23]. Since VNS decreases the production of these cytokines, VNS will thereby potentially inhibit glioma progression[31]. Furthermore, the TME of gliomas consists out of M1 and M2 TAMs, with M2 being the main phenotype[21]. The M2 TAMs are maintained by the expression of NF-κB and will promote glioma progression by the production of pro-tumoral substances. Since VNS results in significant decreased levels of NF-κB, VNS might potentially result in the conversion of M2 TAMs into M1 TAMs and might

suppress glioma progression. Moreover, VNS will result in decreased IL-1β production by the M1 TAMs and thereby inhibit the glioma growth associated pathways of M1 TAMs[31,35]. Considering all the above, VNS could potentially influence the TME and more specific the TAMs by the activation of the cholinergic anti-inflammatory pathway and thereby result in the suppression of glioma progression. Secondly, VNS is an FDA-approved anti-epileptic treatment for medication-resistant epilepsy[36]. The effect of VNS in patients with glioma-related epilepsy is similar to the effect in patients suffering from seizures without a history of brain tumours, resulting in a seizure reduction of at least 50%.

Controversially, the increased levels of GABA in patients and IL-10 within the brain of rabbits observed after receiving VNS, could question the potential therapeutic effect of VNS on glioma growth[29,32]. Firstly, gliomas are characterised by the excessive expression of GABAa receptors[15]. These GABAa receptors are responsible for fast volume reduction of the glioma cells, resulting in the proliferation and migration of glioma cells. Thereby, VNS could enhance glioma progression by his increased GABA levels observed in the CSF of VNS patients. Secondly, TAMs play a crucial role in the hypothesis that VNS could influence glioma progression as mentioned above. Since VNS is mentioned to enhance IL-10 levels in rabbits suffering from a traumatic brain injury, VNS could possibly activate the M2 TAMs[22,32]. These M2 TAMs are known to enhance tumour progression by releasing pro tumoral substances[21]. But VNS can also be responsible for the conversion of M2 TAMs into M1 TAMs by the inhibition of NF-κB. Therefore, the possible increased activation of M2 TAMs by releasing IL-10 can be counteracted by the increased inhibition of NF-κB.

In conclusion, VNS can form a potential treatment for glioma-related epilepsy by targeting tumour progression and epileptic seizures as hypothesized above. VNS could form a treatment without influencing the quality of life of the patients. This hypothesis was investigated as a first part of this master thesis by applying VNS in a GB-related epilepsy rodent model.

5. Low-Grade glioma rodent model

Since patients with LGGs are more vulnerable for the development of epileptic seizures (50-90%) and these patients have a prolonged overall survival, an LGG model is desirable for further research on alternative treatments[2,8]. Since LGG animal models barely exist and are mainly not reproducible or miss the host immune reactions against tumour presence by their immunocompromised character and this often results in an *in vivo* progression towards HGG, the establishment of an LGG rodent model was attempted as a second part of this master thesis[37,38]. Therefore, two different patient-derived paediatric LGG cell lines, Res186 and Res259, were used.

In general, clinical manifestations in patients with LGGs can be divided into two different groups[39]. Firstly, generalizing symptoms develop due to increased intracranial pressure resulting in headaches, vomiting, nausea and lethargy. Secondly, localizing symptoms manifest including seizures, focal neurological deficits and endocrinopathies depending in the localisation of the tumour.

5.1 Res186: Pilocytic Astrocytoma grade I

Res186 cells are isolated out of paediatric pilocytic astrocytoma (PA) in a 3 year old female and are classified as WHO grade I glioma cells. PA are responsible for approximately five percent of all gliomas and are most prevalent in children and young adults[40]. These gliomas occur mainly in children from 5 to 19 years old with a peak incidence from five to nine year[39]. PA occur in different areas within the central nervous system including the cerebellum, optic pathway and hypothalamus[39]. These tumours are characterized by a well-circumscribed growth, low to moderate cellularity and a biphasic grow pattern. This biphasic growth pattern includes the presence of compacted bipolar cells with Rosenthal fibres, eosinophilic fibrillary aggregates, and areas containing multipolar cells, microcysts and eosinophilic granular bodies. PA often possess a large cystic component and an enhancing mural nodule (Figure 9). In addition, the Res186 cell line is defined by a doubling time of 46 hours when cultured in ideal circumstances *(ExPASy, Bioinformatics Resource Portal, cellosaurus).*

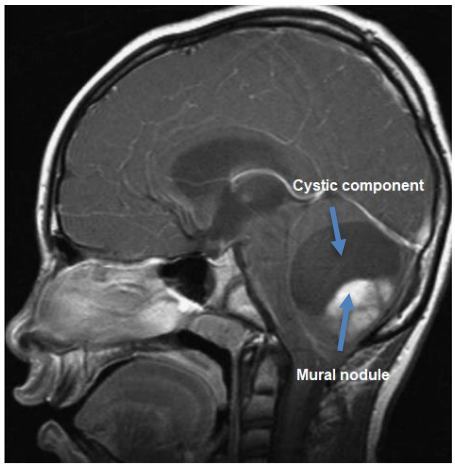

Figure 9. Cerebellar pilocytic astrocytoma T2 weighted MRI. Image from Sievert and Fischer, 2009.

5.2 Res259: Diffuse astrocytoma grade II

The Res259 cell line is isolated out of 4 year old female suffering from a paediatric diffuse astrocytoma, this tumour is classified as a grade II glioma by the WHO[41]. Diffuse astrocytomas present themselves with headache, epileptic seizures and depending on the localisation of these tumours certain neurological deficits *(UCSF Brain Tumour Center*). Furthermore, diffuse astrocytomas are the second most prevalent gliomas after GB with a median survival of five to eight years *(UCSF Brain Tumour Center*)[42]. Additionally, these LGGs have a high recurrence risk due to their diffuse infiltration pattern into the brain and inherent malignant potential to transform towards high-grade astrocytic tumours such as GB.

Diffuse astrocytomas show a pronounced heterogeneity which makes it challenging to grade these tumours based on their histopathological diagnosis[42]. In histology diffuse astrocytomas are characterized by increased cellularity, little nuclear atypia, low mitotic activity, absence of necrosis and microvascular proliferation. Furthermore, formation of “secondary structures of Scherer” including perineuronal satellitosis, subpial growth and perivascular spread take place within these tumours. In addition, the Res259 cell line is characterised by a doubling time of 24 hours when cultured *(ExPASy, Bioinformatics Resource Porta, cellosaurus).*

5.3 Markers for low-grade gliomas

The above described LGG cell lines Res186 and Res259 can be characterized and distinguished from HGG gliomas such as F98 cells using immunocytochemistry staining. Three different markers can be used, glial fibrillar acidic protein (GFAP), vimentin and nestin. Firstly, GFAP is an intermediate filament which is responsible for the cytoarchitecture and the mechanical strength of astrocytes[43]. Furthermore, GFAP is a regularly used marker for reactive astrogliosis, like seen at the tumour border of patients with GB and for mature astrocytes[43,44]. GFAP expression has a significant effect on astrocyte properties, such as morphology, cell-growth and division[44]. In literature, GFAP expression was significantly higher in LGGs than in grade IV gliomas and was negatively correlated with glioma grade. Even more, the expression of GFAP in grade IV gliomas can be less than in healthy brain tissue. Therefore, the expression of GFAP can be used as marker for the astrocytic origin of glioma cells and for the low-grade characteristics of the Res186 and Res259 cell lines during immunocytochemistry staining. Secondly, vimentin is an intermediate filament type III and typically expressed by astrocytes and cells who undergo epithelial to mesenchymal transition (EMT) which is associated with

tumour invasiveness and motility[45,46]. Vimentin is a part of the cytoskeleton and responsible for the maintenance of cellular integrity and the protection of the cells against mechanical stress[45]. This together with the fact that vimentin is an EMT biomarker, suggests that vimentin expression is closely associated with the malignant processes of CNS tumours. In literature, vimentin expression was positively correlated with glioma grade. Therefore, vimentin can be used as an astrocytic marker and high expression patterns are expected in the HGG cell lines such as F98. Thirdly, nestin can be used as marker for HGG. Nestin is an intermediate filament type IV protein involved in the control of cell morphology, adhesion and proliferation and is therefore typically expressed in proliferating and migrating cells[47]. Therefore, nestin is usually used as a stem cell marker. Furthermore, when differentiation starts, cells will exit the cell cycle and nestin expression will be downregulated and alternative intermediate filaments such as GFAP in glial precursor cells will be upregulated. In literature, nestin expression was observed in different brain tumours such as PA and GB[47]. Furthermore, high nestin expression was observed in high malignant tumours (for example GB) when compared to less anaplastic glial tumours. Therefore, nestin can be used as a marker for HGG and a higher expression of nestin is expected in the F98 cell line when compared to the Res186 or Res259 cell lines during immunocytochemistry staining. In the end, the expected results of the three cell lines and the above markers are illustrated in Table1.

Marker	Res186 (Grade I)	Res259 (Grade II)	F98 (Grade IV)
GFAP	High expression	High expression	Lower expression
vimentin	Lower expression	Lower expression	High expression
nestin	Lower expression	Lower expression	High expression

Table 1. Expected expression pattern of the different cell lines and the chosen markers compared to each other.

1. Feasibility to perform VNS in a GB-related epilepsy rodent model

1.1 Cell culture

The F98 rat GB cells (ATTC) were cultured as monolayers in Dulbecco's Modified Eagle Medium (DMEM) in T75 falcons. The DMEM medium (flaks of 500ml) was supplemented with 10% fetal calf serum (FCS), 1% penicillin-streptomycin and 1% of L-glutamine (all products were purchased from Invitrogen®). Fetal calf serum or fetal bovine serum is essential in cell cultures because it contains a large amount of nutritional and macromolecular factors essential for cell growth and a smaller amount of antibodies than non-fetal serums[48]. Furthermore, 1% penicillin-streptomycin was added to prevent bacterial contamination by their combined action against gram-negative and -positive bacteria. The concentration of penicillin is 10 000 units/ml and for streptomycin 10 000µg/ml. Also 1% of L-glutamine was added to participate in the formation of amino acids, protein synthesis and glucose production. Furthermore, the DMEM contains a Phenol red indicator which is used as a pH indicator. Thereby, the DMEM will turn yellow when the pH drops below 6.8 (acid) and pink when the pH exceeds 8.2 (base). Since acidic and basic environments are unfavourable conditions for cell culturing this Phenol red indicator was crucial in monitoring the cell cultures. The cell cultures were maintained in an incubator at 37°C and in 5% CO_2 and were split when 80% confluency was reached (illustrated in addendum section *1. Cell passage*).

During the preparation of 20 000 F98 cells in 5µl PBS for inoculation, a Bürker chamber was used to count the correct number of cells. Firstly, a cell suspension was obtained via the first four steps of cell passage; taking off the DMEM medium, washing the cells with PBS, adding 2ml of trypsin and letting it incubate for 5 minutes and adding 2ml of DMEM as illustrated in the addendum section *1. Cell passage*. Thereafter, 50µl of the cell suspension was taken out and 50µl of trypan blue was added in order to stain the death cells, meaning the cell suspension was ½ diluted. Then, the cells were counted three times in the Bürker chamber and the mean was calculated. For the number of cells in 1ml, the mean was multiplied by two (due to the dilution of ½) and 10 000 (the volume in one square is 100nl or 0.0001ml). Once the number of cells in 1ml was known, the correct volume of cell suspension was calculated in order to have 2 000 000 F98 cells. This volume of cells suspension was centrifuged, the liquid was taken off and the cells were diluted in 500µl phosphate buffered saline (PBS). Resulting in a final concentration of 20 000 F98 cells in 5µl PBS. The cells were prepared right before inoculation in order to minimize the amount of death cells injected. A counting error occurred in one animal and only 11 000 cells were inoculated (an estimation of the total amount of cells injected is illustrated in the addendum section *3.4 Tumour volumes of all animals*).

1.2 Animals

Eight male F344/IcoCrl rats (Charles River®) of 10 weeks old were used during this study. The study was approved by the animal ethics committee of the Faculty of Medicine and Health Sciences of Ghent University (ECD 17/111). All animals were kept and handled according to the European guidelines (Directive 2010/63/EU) and housed under environmentally controlled conditions: 12h light/dark cycle, temperature between 21-24°C and humidity between 40-60%.

1.3 Surgery

All animals were anaesthetised with a mixture of medical oxygen (rate: 1l/min) and isoflurane (induction: 5%; maintenance: 2%). At the start of surgery all animals were weighted and blood samples from the tail were collected. The blood samples were collected by heating the tail using an infrared lamp in order to make the tail veins visible. Next, a winged intravenous catheter was put into the tail vein and the blood was captured in a sterile Eppendorf tube of 1.5ml. Maximum 0.6ml blood was collected from each animal. Thereafter, the animals were implanted with a VNS electrode around the left vagus nerve. After implantation of the VNS electrode, animals were immobilized in a stereotaxic frame, EEG registration electrodes were

implanted and 20 000 F98 cells in 5µl PBS were inoculated into the right entorhinal cortex. During surgery the body temperature was maintained at 37°C using a heating pad and this was controlled by rectal measurement every 30 minutes.

1.3.1 VNS implantation

Before implantation of a 'custom-made' VNS electrode (described by El Tahry *et al.* [49]) which consisted out of an anode(+) and a cathode(-), the impedance was tested and only VNS electrodes with an impedance between 2-5kΩ were used. At the start of the surgery, animals received a subcutaneous injection of Vetergesic® (0.1 ml from a concentration of 0.03mg/ml). Then the head and neck region (from the chin till the forelimbs) were shaved using soap (Hibiscrub®) and water. The animals were placed on their back on a heating pad and a nose cone was used to deliver the mixture of medical oxygen (rate:1.2l/min) and isoflurane (2%). The shaved neck region was disinfected using iso-Betadine® before a medial incision, ranging from the sternum to the chin, was made. Next, the skin was separated from the tissue and tissue was removed from the fused glands using forceps. The two fused glands (Figure 10 a.) were separated in order to expose the triangle point of three muscles (m. sternocleidomastoid and the omohyoid muscles) located at the left. Thereafter, the left vagus nerve (recognized by its striped ladder pattern) was isolated from the carotid sheath and carotid artery. Once the left vagus nerve was properly isolated, the VNS electrode was wrapped around the vagus nerve with the anode placed caudally (Figure 10 b.) and saline was applied immediately. The muscles were placed back over the vagus nerve followed by the glands which were stitched together (Figure 10 c.). Then the leads of the VNS electrode were placed underneath the stitched glands and an additional stitch was added above the leads (Figure 10 d.). The remainder leads were tunnelled subcutaneously to the head. At the end of this procedure the neck region was sutured.

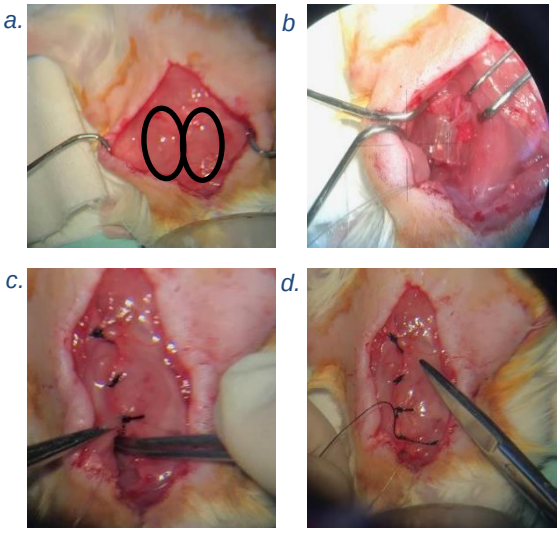

Figure 10. a. The two fused glands seen during surgery. b. The VNS electrode is wrapped caudally around the left vagus nerve. c. The glands are stitched together and the leads from the VNS electrode are partly put underneath the glands. d. An extra stitch is made between the glands.

1.3.2 Inoculation and implantation of EEG electrodes

After the implantation of the VNS electrode, the animals were immobilized using a stereotaxic frame (Figure 11) and anaesthesia was lowered to 1.5% isoflurane and a medical oxygen rate of 0.8ml/min. Iso-Betadine® was applied to the shaved head and a subcutaneous injection of adrenaline/xylocaine (0.1ml of the solution containing 20mg/ml lidocainehydrochloride, xylocaine 2% and adrenaline 1:200 000) was given right above the skull. Thereafter an incision was made to expose the skull. Firstly the skull was hatched to make it rougher, then acetone was applied to destroy the periost and make the sutures more visible, next green activator was applied for an optimal functioning of later applied Metabond® and lastly saline was applied in order to rinse off the green activator (result illustrated in Figure 12). The coordinates of Bregma and Lambda were defined to check whether the skull was positioned correctly and in order to determine the inoculation site and

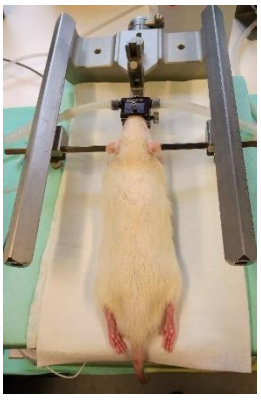

Figure 11. Rat immobilized in a stereotaxic frame.

Figure 12. Result of the skull after hatching, applying acetone, green activator and saline.

coordinates for the bipolar depth-electrodes as accurate as possible. This was followed by the implantation of scalp electrodes and anchor screws. Firstly, burr holes of 1.1mm were made for the type I screws; two traumatic scalp electrodes consisting of type I screws were placed in the os frontale functioning as ground and spare ground, and three type I anchor screws were placed in the os occipitale (Figure 13). Secondly, burr holes of 0.9mm were made for the type II anchor screws and an atraumatic scalp electrode consisting of a type II srew. The atraumatic scalp electrode, to record surface EEG, was placed over the right parietal cortex, near the tumour border and medial-posterior from the right bipolar depth-electrode (Figure 13). Two type II anchor screws were placed in the os frontale and one in the os parietale (Figure 13). Traumatic and atraumatic scalp electrodes differ in shape of the extremity of the screw for attachment in the skull. An type II screw contains a flat end with screw thread covering the whole tip, whereas type I screws have rounded tips without screw thread. Type I screws have a better fixation but will reach deeper through the skull when attaching them and therefore these screws are more likely to cause damage to the cortex. This will be prevented by using type II screws. Thus, type II screws were used above cortical areas, to avoid damage to the cortex and the risk of provoking seizures, since this trial investigated glioma-related seizures. After placements of the anchor screws and the scalp electrodes, Metabond® was applied around the screws in order to secure the attachment of the screws to the skull and to secure the dental cement that was used at the end to make the head cap.

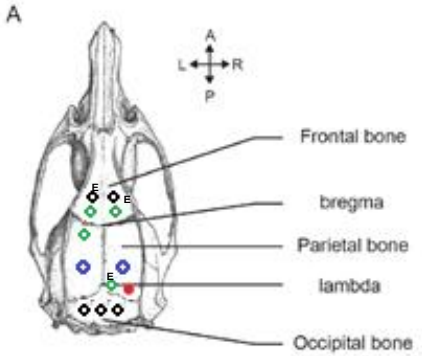

Figure 13. Rat Skull. Brunner, Clément. (2016). Type I screws are black and type II screws green. The scalp electrodes are indicated with an E abbreviated from electrode. The bipolar depth-electrodes are presented in blue. The inoculation place is marked in red.

Then a craniotomy for inoculation was made 8mm posterior and 4.5mm right to Bregma. Next, an insulin needle (BD 0.5 ml Insulin Syringe Microfine 0.33 mm (29G) x 12.7 mm) was filled with the F98 cell suspension and mounted on a pump for automatic injection (Stoelting Quintessential Stereotaxic Injector (QSITM), Stoelting Co.). The insulin needle was stereotactically guided to the right coordinates relative to bregma (anteroposterior (AP): -8.0mm; mediolateral (ML): +4.5mm). Then the insulin needle was inserted through the craniotomy to a depth of -4.1mm relative to dura in order to inoculate the cells in the right entorhinal cortex. 20 000 F98 cells in 5µl of PBS were injected over a time period of 10 minutes and the syringe was kept in place for five minutes post-inoculation and thereafter slowly removed. In this study, the inoculation day was referred to as day 0.

After the inoculation two craniotomies for the bipolar depth-electrodes (Figure 13) were made (AP: -5.0mm; ML: +/- 3.5mm relative to bregma). Bipolar depth-electrodes were custom-made and the tips were 0.9mm apart in order to simultaneously record activity in the dentate gyrus and the CA1 region of the ipsi- and contralateral hippocampus. Via a small incision in dura the depth-electrodes were lowered in the brain 3.5mm below dura. The electrodes were fixed to the skull and neighbouring anchor screws using UV-cement (Filtek Supreme XTE Plus Flowable 2 x 2 gr, 3M, Belgium). The leads of the VNS, scalp and depth-electrodes were assembled in a head cap on the skull of the rat using resin-based dental cement (Simplex Rapid fluid/powder, Kemdent, UK). At the end of the surgery the scalp was sutured, Metacam® (1ml/kg) and 1ml of saline were administered subcutaneously. The animals were transferred to their cages and one DietGel® Recovery was given to each animal for fast recovery. Furthermore, animals were inspected daily.

1.4 EEG monitoring and VNS stimulation

Six animals were connected to the EEG setup at day 7. They were anaesthetized with a mixture of medical oxygen and isoflurane (induction: 5%; maintenance: 2%), a second blood sample was taken (as described in 1.3) and thereafter they were connected to the EEG setup.

The EEG setup consisted out of a head stage carrying a 4-channel unity gain amplifier (based on a TL074 SMT Opamp, Texas Instruments, Dallas, TX, USA) that is connected via tethers to a 12-channel commutator (Plastics One, Roanoke, VA, USA) allowing the animals to move freely. The commutator is connected to a custom-made 4 channel high pass filter with a time constant of 1 second followed by a 4-channel 512 x amplifier (based on TL074 Opamp) and a NiDAQ to digitize the signal (USB-6259, National Instruments Device). Stimuli to the left vagus nerve were delivered via an external constant current stimulator.

For VNS stimulation the animals were *ad random* assigned to the SHAM or VNS group and only the VNS group received stimulation. Both groups consisted out of three animals; the animals belonging to the VNS group were the 1st, 2nd and the 3rd VNS rat and the animals belonging to the SHAM group were the 1st, 2nd and 3rd SHAM rat. In the VNS group the impedance of the electrode was measured before stimulation was started using an oscilloscope. Impedance should be below 10 kΩ. The VNS group was stimulated with the following parameters: 30Hz, biphasic pulses of 250µs/phase, 0.5sec ON/29.5sec OFF as illustrated in Figure 14. The VNS stimulation was gradually increased in steps of 250µA from 250µA at day 10 to 1mA at day 13. According to previous research, VNS can induce hypothermia [50]. Therefore, the parameters above were chosen because they were not related to any hypothermia in rats[51].

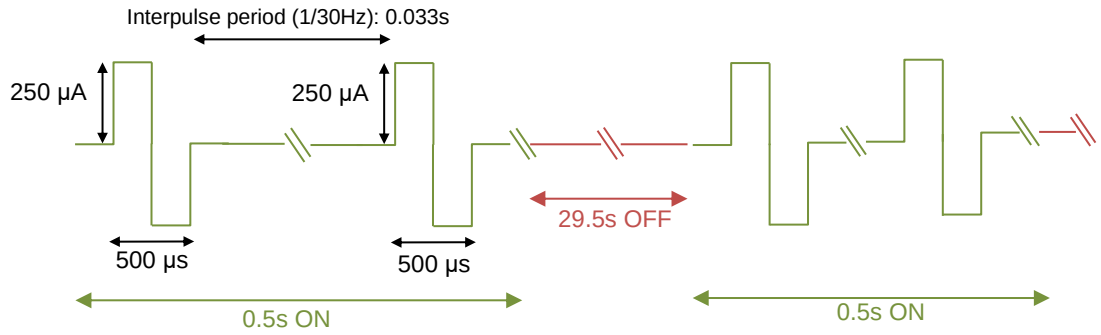

Figure 14. VNS stimulation protocol.

1.5 Perfusion

All animals were transcardially perfused at day 14 and the brains were snap frozen in liquid nitrogen. The animals were first anaesthetised with a mixture of medical oxygen and isoflurane (induction: 5%; maintenance: 2%) and blood samples were taken (as described in 1.3). This was followed by an overdose of sodium pentobarbital (200mg/kg) which was injected intraperitonially. From the moment the animals stopped breathing they were transcardially perfused. The chest was opened and the beating heart was carefully isolated out of the pericardium. Firstly, 0.1ml of heparin was injected into the apex of the beating heart to avoid blood clotting. Secondly, a needle was placed through the apex into the aorta and a cut was given in the right atrium. Next, the veins were flushed with saline at room temperature for one minute followed by ice cold PBS till the no more blood was present in the liquid coming out of the right atrium (Figure 15). After transcardial perfusion, the brains were isolated. Immediately thereafter the brains were put into liquid nitrogen and stored until histology.

Figure 15. Transcardial perfusion of a rat.

1.6 Blood samples

After taking the blood samples, these were kept at room temperature for at least 15 minutes. Then, the samples were centrifuged for 10 minutes at 14Hz in order to fraction the blood into serum (the upper fraction) and the clotted blood (the lower fraction). In the end, 100µl serum was collected in a marked sterile Eppendorf tube of 1.5ml using a micropipette (0-100µl) and stored in the -80°C freezer. If possible three tubes of serum per blood sample were collected.

Serum was collected to check for inflammatory markers TNF-α, NF-κB, IL-6 and IL-1β. These inflammatory markers were chosen to investigate whether the potential effect of VNS on tumour growth and related seizures were related to the effect of VNS on inflammation. At day 7 increased levels of the serum levels of IL-6, IL-1β and TNF-α are expected as these cytokines are correlated with glioma grade and clinical invasiveness of GB and tumour growth is expected in all animals[52]. Controversially, the samples collected at day 14 were expected to be different between the VNS and SHAM group, since VNS could influence glioma progression and related seizures in the VNS group together with inflammation[31]. The serum level of IL-6 is strongly related with seizure occurrence and severity, since more seizures are expected in the SHAM group compared to the VNS group, increased levels of IL-6 are expected in this group compared to baseline[53,54]. Serum levels of IL-1β, IL-6 and TNF-α are expected to be decreased in the VNS group since VNS can potentially inhibit glioma progression and these cytokine levels are positively correlated with GB invasiveness[52].

1.7 Histology

Tumour volumes were determined on tumour-containing cresyl violet-stained coronal sections with a thickness of 5µm. Before coronal sections were made, the brains had to be transferred from the liquid nitrogen into the -20°C freezer for at least two hours. Then coronal sections of 5µm thickness were made using a cryostat (Leica, Germany). Therefore, the frontal part of the brain was cut off, placed on the cryostat holder and embedded in optimal cutting temperature compound. Thereafter, 5µm-thick slices were made. Starting from the slice where the tumour was observed or suspected three succeeded consecutive slices were mounted directly on a glass slide. This procedure was repeated every 100 slices until no more tumour tissue was observed. One additional glass slide was made 100 slices further to ensure the slices covered the whole tumour.

Before calculation of the tumour volumes, cresyl violet staining was performed. In order to perform a cresyl violet staining, the slices were dried overnight at room temperature. First, the slices were put in the cresyl violet acetate solution for 10 minutes. Cresyl violet acetate is a basic dye which attracted the extracellular RNA granules and stains it blue due to RNA's basophilic properties. This way, the tumour cells could be indicated by a darker blue due to their higher amount of extracellular RNA. Secondly, the slices were rinsed in distilled H_2O. Thereafter, the slices were put in 96% ethanol for 1minute and 30seconds. This step is called the differentiation step and is necessary to remove excess staining. Next, the slices were put in 100% of ethanol for five minutes and this was done two times. These steps functioned as dehydration steps to minimize the discolouring or precipitating effect of the hydrophobic xylene. Thereafter, the slices were put in xylene twice, for five minutes. Since the mounting medium contained toluene, xylene was used to remove all hydrous compounds in order to minimize air bubbles when coverslipped. Finally, one droplet of Entellan® mounting medium was applied to each slice and a coverslip was put on the glass slide, air bubbles were removed and the slices were dried overnight.

After the cresyl violet staining, the slices were scanned using a light microscope. The best slice was selected on each glass slide, the tumour border was aligned and the surface area was calculated using ImageJ (Figure 16). The surface area of each selected slice was multiplied by 0.5mm because each calculated surface area represented the mean of 100 slices of 5µm. In the end, the final tumour volume of each animal was estimated by the sum of all calculated volumes.

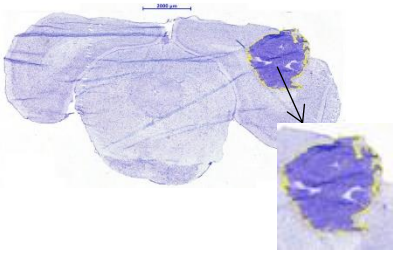

Figure 16. Aligned tumour border in ImageJ. The tumour is represented by a darker stained area.

2. Low-grade glioma

2.1 Cell culture

The Res186 (human pilocytic astrocytoma, grade I) and Res259 (human diffuse astrocytoma, grade II) cells were cultured as monolayers in DMEM/F-12 Ham's medium in T75 falcons. The DMEM/F-12 Ham's medium was enriched with 10% FCS, 1% penicillin-streptomycin and 1% of L-glutamine (all products were purchased from Invitrogen®). The cell cultures were maintained in an incubator at 37°C and in 5% CO_2 and split when 80% confluency was reached.

For immunocytochemical staining and further characterisation of the cells, the cells were fixated on glass slides. Also, the F98 cells (cultured as described in *1.1 Cell culture*) were fixated on glass slides. Therefore, the cells were first cultured in a petri dish containing a glass slide for 24hours in the incubator (37°C and 5% CO_2). Thereafter, the medium was taken off and the glass slide was rinsed with PBS two times. This was followed by the incubation of the glass slide in paraformaldehyde (PFA) for three to five minutes in the incubator in order to fixate the cells. Then the glass slide was again rinsed in PBS (three times) and dried to the air. In the end, the glass slides were stored in the -20°C freezer and ready for immunocytochemical staining.

2.2 Animals

During *in vivo* experiments in this study four rats were used in order to establish LGG growth: one male F344/IcoCrl rat of nine weeks old, two Sprague Dawley rats of 27 weeks old and one RNu rats (T cell deficient) of eight weeks old. The study was approved by the animal ethics committee of the Faculty of Medicine and Health Sciences of Ghent University (ECD 17/111). All animals were kept and handled according to the European guidelines (Directive 2010/63/EU) and housed under environmentally controlled conditions: 12h light/dark cycle, temperature between 21-24°C and humidity between 40-60%.

2.2.1 Non-immunocompromised rats

The F344/IcoCrl rat (1st normal rat)and the two Sprague Dawley rats (2nd and 3rd normal rat) were used. Due to the human origin of the Res186 (grade I) and the Res259 (grade II) cell lines, it was supposable that the cells would not grow in these rats due to an immune mediated rejection in response to their human origin. Nonetheless, the 20 000 grade I or grade II cells in 5µl PBS were inoculated in the right entorhinal cortex of these animals because immunocompromised rats are not 100% representative for the mechanisms and responses against potential therapeutics in patients[55]. The entorhinal cortex was chosen due to its high susceptibility for epileptic seizures as the goal of this study was to establish an LGG-related epilepsy rodent model. However, at first only the growth possibility of these cell lines was explored in these non-immunocompromised rats.

The 1st and 2nd normal animals were inoculated with 20 000 grade II cells in 5µl PBS and the 3rd normal animal was inoculated with 20 000 grade I cells in 5µl PBS. Cell counting was

performed as described in section *1.1 Cell culture*. The animals were anaesthetized using a mixture of medical oxygen (induction: 1l/min; maintenance: 0.8ml/min) and isoflurane (induction: 5%; maintenance: 2%). First, the head was shaved using water and soap (Hubiscrub®) and disinfected with iso-Betadine®. Next, the animals were immobilized using a stereotactic frame and lidocaine was put on the ear bars to minimize pain. Then a subcutaneous injection of adrenaline/xylocaine (0.1ml) was given right above the skull and an incision was made to expose the skull. Next, the coordinates of Bregma and Lambda were determined to check whether the skull was positioned correctly. Then the 20 000 grade I or II cells in 5µl PBS were inoculated in the right entorhinal cortex as described in section *1.3.2 Inoculation and implantation of EEG electrodes*. In this study, the inoculation day was referred to as day 0. The animals were followed up and weighted daily.

The animals were transcardially perfused on day 14 (as described in section *1.5 Perfusion)*. Tumour growth was already expected on day 14 as the LGG cell lines had respectively longer doubling times *in vitro* (24 hours for Res259 and 46 hours for Res186) than the F98 cell line (13 hours) and are therefore expected to grow slower *in vivo* as well (*ExPASy, Bioinformatics Resource Porta, cellosaurus)*[34]. Moreover, large tumour volumes were already observed in the GB-related epilepsy rat model on day 14[33].

2.2.2 T cell deficient rats

Since the human LGG cell lines (grade I and grade II) are not easily grown *in vivo*, tumour growth was thought to be acquired more easily in T cell deficient Rowett Nude (RNu) rats than in non-immunodeficient rats. One RNu rat was inoculated with 20 000 grade I cells in 5µl PBS and 20 000 grade II cells in 5µl PBS respectively in the left and right entorhinal cortex.

For the inoculation of 20 000 grade I and 20 000 grade II cells, cell counting was performed as described in section *1.1 Cell culture.* Thereafter, the animal was anaesthetized using a mixture of medical oxygen (induction: 1l/min; maintenance: 0.8ml/min) and isoflurane (induction: 5%; maintenance: 2%) and extra safety measurements were taken to protect the T cell deficient rat, such as wearing sterile gloves and a mask. The protocol of the surgery was the same as described in section *2.2.1 Non-immunocompromised rats*. But this animal was inoculated at both sides. The coordinates of the craniotomies were respectively 4.5mm right to Lambda for the grade I cells and 4.5mm left to Lambda for the grade II cells. The coordinates of Bregma could not be precisely determined. Since the distance between Bregma and Lambda is almost 8mm and the inoculation site is determined 8mm posterior and 4.5mm mediolateral from Bregma, Lambda could be used as reference to mark the inoculation site only based on the medio-lateral coordinates. The other parts of the surgery were equal as described in section *2.2.1 Non-immunocompromised rats.*

The animal was followed up daily and weighted until day 54. Furthermore, potential tumour growth was followed up using T2-weighted magnetic resonance imaging (MRI) scans on day 10, 14, 31 and 66 with a 7-tesla micro MRI (PharmaScan 70/16, Bruker BioSpin, Ettlingen, Germany). Abnormal tissue such as tumours are hyperintense on T2-weighted MRI scans. 109 days after the inoculation, the animal was transcardially perfused due to the Sars-CoV-2 pandemic. This was a transcardial perfusion as described previously (section *1.5 Perfusion*) but PBS followed by 4% PFA were used instead of saline at room temperature and ice-cold PBS respectively. The brain was isolated and stored in 4% PFA at 4°C in order to perform *ex vivo* MRI on later time points.

2.3 Histology

2.3.1 Immunocytochemistry

The two LGG cell lines and the HGG F98 cell line were stained with an immunocytochemistry staining. Three different markers were used to confirm low-grade characteristics of the Res186 (grade I) and Res259 (grade II) cell lines and to distinguish LGG cell lines from the HGG cell line: glial fibrillar acidic protein (GFAP), vimentin and nestin. Firstly, the expression of GFAP

was used as a marker for the astrocytic origin of the glioma cells and for the low-grade characteristics of the grade I and grade II cell lines during this immunocytochemistry staining. Secondly, vimentin was used as an astrocytic marker and a high expression pattern was expected in the F98 cell line. Thirdly, nestin was used as a marker for HGG and a higher expression of nestin was expected in the F98 cell line compared to the grade I or grade II cell line during immunocytochemistry staining. A brain slice containing a F98 tumour was used as control during the immunocytochemistry staining. This control is known to be positive for GFAP and vimentin. In the end, the expected results for the three cell lines are illustrated in Table1.

Immunocytochemistry staining was performed on the glass slides containing the fixed F98, grade I and grade II cells. The glass slides were first treated with 0.5% and 1% H_2O_2 for 30 and 60 minutes respectively to block the endogenous peroxidase activity. Thereafter, the cells were washed for two times with PBS. These steps were followed by an incubation of blocking solution containing PBS, 0.2% Triton X-100 and 0.4% Fish Skin Gelatine for 45 minutes in order to block non-specific binding of the primary antibodies. Next, the primary antibodies were applied for one hour at room temperatures at the following dilutions: rabbit anti-GFAP 1:1000 (DAKO, Heverlee, Belgium), mouse anti-vimentin 1:250 (DAKO, Heverlee, Belgium) and mouse anti-nestin 1:500 (Santa Cruz Biotechnology, Dallas, United States). Then, the blocking solution was again applied to the cells for two times 10 minutes and the secondary antibodies labelled with a fluorescence tag were applied in the dark for one hour at room temperature with the following dilutions: goat anti-mouse Alexa fluor 488 1:1000 and anti-rabbit Alexa fluor 594 1:1000 (all secondary antibodies were purchased from DAKO). Next, the cells were rinsed with PBS two times, DAPI was applied for one minute to stain the cell nuclei and again rinsed with PBS for two times all in the dark. Finally, three droplets of Fluoroshield™ histology mounting medium were applied per glass slide and glass slides were covered with a cover glass making sure most of the air bubbles were removed.

In total, two glass slides with grade I cells, two with grade II cells and only one with F98 cells were stained. One of the glass slides with the grade I and grade II cells was stained for GFAP/nestin and the other one for GFAP/vimentin. This way it was possible to use the same secondary antibody for nestin and vimentin namely anti-mouse Alexa fluor 488. The F98 glass slide was only stained for GFAP/nestin due to the Sars-CoV-2 pandemic. In the end, a fluorescence light microscope was used to analyse the expression of the different markers in the cells and the cell nuclei. This was feasible due to the fluorescent secondary antibodies that were used during this immunocytochemistry staining, the anti-rabbit Alexa fluor 594 which turned red by illumination of light with a wavelength of 594nm and the anti-mouse Alexa fluor 488 which turned green by illuminated of light with a wavelength of 488nm (Figure 17).

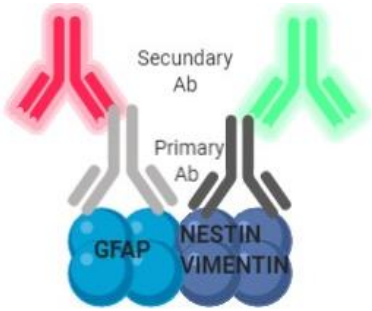

Figure 17. Theoretic illustration of immunocytochemistry staining on the different cell lines. Image created using BioRender.

2.3.2 In vivo low-grade glioma model

Before coronal sections were made, the brains had to be transferred from the liquid nitrogen into the -20°C freezer for at least two hours. Then, coronal sections of the brains of the control animals were made using a cryostat (Leica, Germany). The frontal part of the brains was cut off, brains were put onto the cryostat holder and coronal slices with a thickness of 5µm were made. The slices from the 1st and 2nd normal rat were collected as described in section *1.7 Histology* from the moment tumour was expected, just after the injection site. For the 3rd normal rat the suspected tumour slices were mounted directly on glass slide without applying the procedure as mentioned above. Some glass slides containing additional slices around the inoculation site were kept in the -80°C freezer to perform later immunohistochemistry staining if tumour presence was confirmed on cresyl violet stained slices.

Tumour presence was evaluated using cresyl violet staining on the collected slices. The slices mounted on the glass slides were first dried overnight at room temperature. Then a cresyl violet staining was performed as described in section *1.7 Histology*. After staining, pictures of the stained slices were made using a light microscope and analysed for tumour presence.

RESULTS

1. Feasibility of VNS in a glioblastoma-related epilepsy rodent model

1.1 VNS stimulation and EEG analyses

From day 7 until day 14 the brain activity of the animals was monitored using EEG. Before the animals were connected to the setup for continuous EEG monitoring, one animal died at day 6 and another animal was euthanized after having clear breathing problems on day 5. Furthermore, one animal of the VNS group (VNS rat 3) developed a progressing wound on his tail after the second blood sample was taken. Therefore, Neo-Cutegenol® was applied to the wound twice a day. As this was not sufficient, subcutaneous injections of Metacam® (0.2ml/kg), Baytril® (10mg/kg) and 1ml of saline were administered daily from day 10 until day 13. The animal also received extra calories by a DietGel® Recovery.

The impedance of the VNS electrode in all VNS animals was between the 2-4kΩ before the start of VNS at day 10. No seizures were detected during baseline EEG monitoring. Two seizures were detected in one VNS animal (VNS rat 2) during the stimulation period, on day 12 (duration 143s) and day 13 (duration 164s) post-inoculation (Figure 18). In the other animals no seizures were detected. However, no EEG data of the second part of day 13 and day 14 until euthanasia were available in two SHAM animals (SHAM rat 2 and 3)due to a technical error.

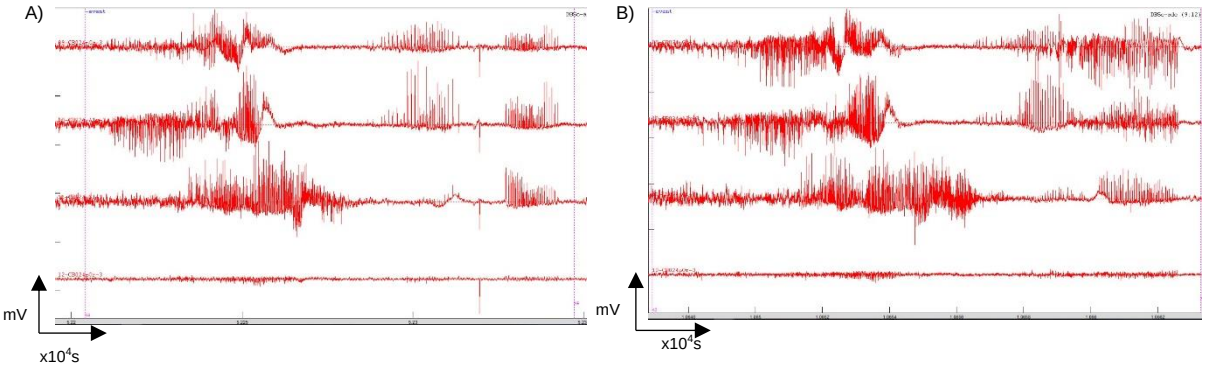

Figure 18. Seizures of the 3rd VNS animal. A) illustrates the first seizure of 143 seconds. B) illustrates the second seizure of 164 seconds.

1.2 Histology

Cresyl violet staining was used to calculate the GB volumes of all the rats (n=6). When the slices were made, problems occurred in three animals (VNS rat 3, SHAM rat 2 and 3). On the cresyl violet staining it was clear that tumour tissue was lacking in several slices. Therefore, these three animals (VNS rat 3, SHAM rat 2 and 3) were excluded to draw conclusions about the effect of VNS of tumour volume. Good slices were obtained from the three remaining rats (SHAM rat 1, VNS rat 1 and 2). The SHAM rat 1 had a tumour volume of 16.96mm^3. The tumour volumes of the VNS animals were remarkedly lower, namely 11.66mm^3 for VNS rat 1 and 8.18mm^3 for VNS rat 2. The mean tumour volume of the VNS animals was therefore 9.92 ± 2.46mm^3. The results of the cresyl violet staining and the calculated tumour volumes are illustrated in the addendum section *4. Tumour volumes*. One remark can be made, during perfusion of the animals with ice cold PBS all the six animals reacted heavily and grinded their teeth.

1.3 Blood samples

The blood samples could not be analysed due to the Sars-CoV-2 pandemic.

2. Low-grade glioma

2.1 Immunocytochemistry

The grade I and II cells did not express any GFAP. The staining for GFAP was repeated two times including a control and still no expression of GFAP was observed. The F98 cells did express a small amount of GFAP (Figure 19).

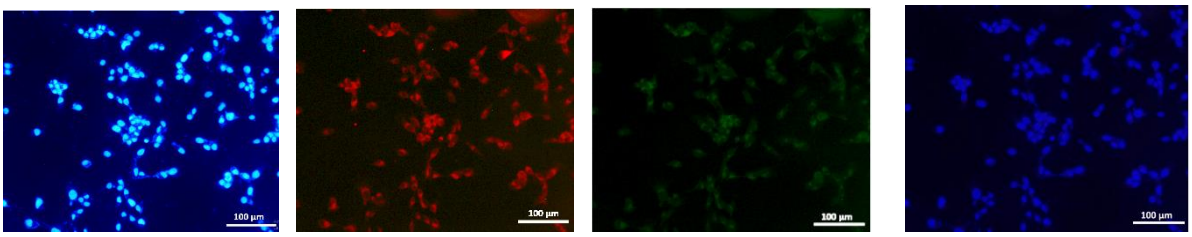

Figure 19. Stained F98 cells. The merged picture is the DAPI +GFAP+ nestin staining.

The grade I and II cells expressed vimentin. Vimentin intermediate filaments were less dense packed in the grade I cells compared to the grade II cells (Figure 20). Furthermore, the F98 cells could not be investigated for vimentin expression due to the Sars-CoV-2 pandemic. No expression of nestin was observed in the grade I cell line and only a very weak expression in the grade II cell line compared to the F98 cell line (Figure 21).

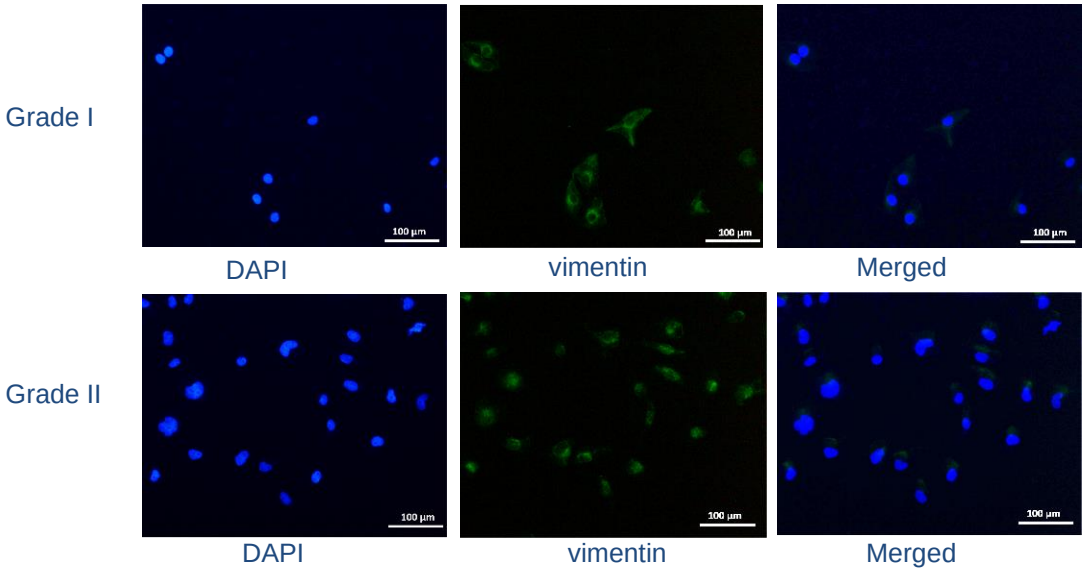

Figure 20. Staining of the grade I and grade I cells. Both cells were negative for GFAP and this staining is therefore not shown.

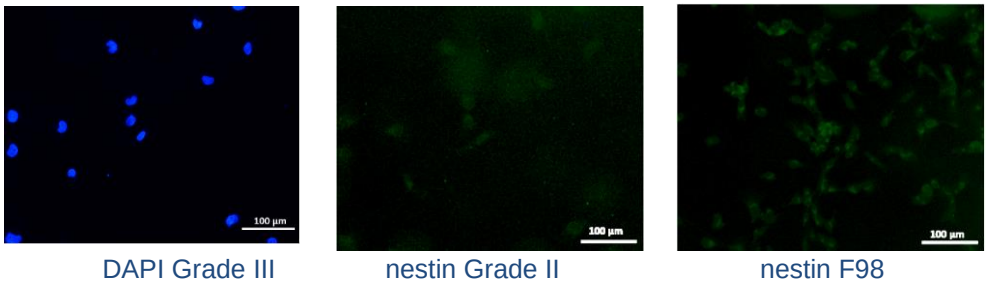

Figure 21. Expression patterns of DAPI and nestin in the Grade II cells. There is only a very weak nestin expression of nestin compared to the F98 cells.

2.2 In vivo low-grade glioma model

2.2.1 Non-immunocompromised rats

In all three non-immunocompromised rats no weight loss was observed during the study (illustrated in the addendum section *2.1.2 Weight follow-up of the animals*) and they were still in good condition right before perfusion (day 14 post-inoculation). During sectioning of the brains, no tumour tissue could be identified. The absence of tumour was confirmed during the analyses of the cresyl violet stained slices (Figure 22). Some errors occurred during snap freezing and sectioning of the brains. Firstly, when the brains were snap frozen, the isolated brain was sometimes put on his side in the cryovial resulting in an unbalance of hemisphere size between left and right. In the 2nd normal rat this resulted in the cerebellum lying on top of the cerebrum. Therefore, the cerebellum was removed from the cresyl violet pictures.

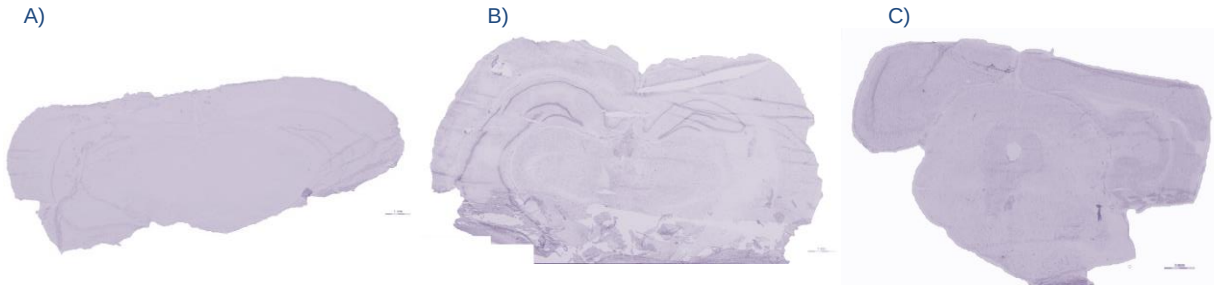

Figure 22. Cresyl violet staining of the control rats. A) The 1st normal rat inoculated with 20 000 grade II cells. B) The 2nd normal rat inoculated with 20 000 grade II cells. C) The 3rd normal rat inoculated with 20 000 grade I cells. In conclusion, no tumours were observed.

2.2.2 T cell deficient rat

The RNu rat did not lose weight over time (illustrated in the addendum section *2.1.2 Weight follow-up of the animals*) and was in good shape when euthanised on day 109. No hyperintense regions were observed on the T2 MRI scans at different time points. The last MRI was performed 66 days post-inoculation and still no tumour was visible (illustrated in figure 23).

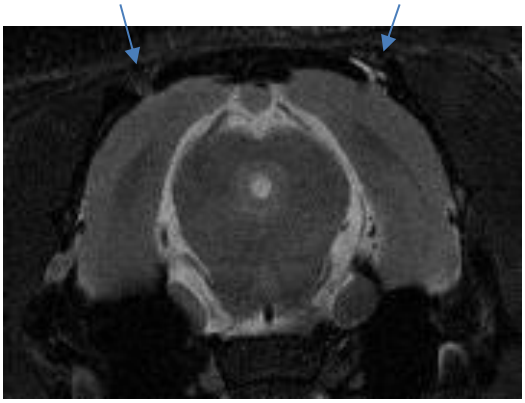

Figure 23. T2 MRI scan of the RNu rat at day 66 at the inoculation sites (illustrated with the two arrows).

DISCUSSION

1. Feasibility of VNS as treatment for glioma-related epilepsy?

Seizures

Only in one animal (VNS rat 2) seizures were observed during this study. Remarkedly, this animal received VNS. A first possible explanation for the manifestation of seizures in this animal (VNS rat 2) is the administration of Baytril® and Metacam® (to avoid bacterial infection on his tail and relieve the pain) since the seizures occurred in the same time frame (day 12 and 13) as administration of the medication (day 10 till day 13). Baytril® is a well-known and often used second generation fluoroquinolone containing enrofloxacin (https://www.baytril.com/en/farm-animals/product/oral/). Fluoroquinolones, mostly newer generations, can evoke side effects in the central nervous system[56]. They inhibit GABA binding to his receptor *in vitro* and can therefore potentially evoke seizures *in vivo*. In addition, drug-drug interactions between non-steroidal anti-inflammatory drugs (NSAID) and fluoroquinolones enhance the inhibition of GABA evoked by fluoroquinolones[56]. Since this animal received Metacam®, an often used NSAID, combined with Baytril® from day 10 until 13 this could be an explanation for the seizures observed in this animal. Furthermore, animals who are suffering from GB have a weakened GABAergic inhibition of the peritumoral cortex and are thereby more vulnerable for the development of seizures[15]. The administration of Baytril® and Metacam® in these animals can enhance the weakening of the GABAergic inhibition of the peritumoral cortex by blocking the GABA receptors[56]. Therefore, these animals can be more vulnerable for the development of seizures, whether or not they received VNS. Secondly, the relationship between GB volume and seizure frequency could be a possible explanation why only in this animal (VNS rat 2) seizures were detected. A smaller HGG volume in patients is related with a higher seizure frequency which can be explained by their rapid tumour growth[57,58]. Since the tumour volume of the 3rd VNS animal (8.18mm³) was less than the tumour volumes of the 1st VNS animal (11.66mm³) and the 2nd SHAM animal(16.96mm³) without seizures, the smaller GB volume could possibly be another reason for the observed seizures in this animal. Additionally, the therapeutic effect of VNS on GB-related seizures can be questioned since the seizures only occurred in a VNS animal. As observed in humans not everybody is a VNS-responder, the VNS response rate increases over time and VNS supresses only 50% of the seizures[29,30]. Since these animals were only stimulated for four days, it is plausible that this animal (VNS rat 2) was a VNS non-responder or VNS was not able to suppress all seizures. Furthermore, the obtained data in this study is not representative for the efficacy of VNS for GB-related seizures due to the lack of seizures in the other animals.

The fact that no seizures were observed in the other five animals can be explained via several arguments. Firstly, the EEG recording was interrupted due to computer problems at the end of the experiment in two SHAM animals (SHAM rat 2 and 3) resulting in the absence of EEG data from the last day. Thereby, seizures cannot be excluded in these animals. Additionally, in one animal (SHAM rat 2) abnormal electrical activity was observed on day 10 but this was not classified as an epileptic seizure. The use of video-EEG monitoring in future experiments can exclude doubtful cases as the one observed in this animal. A general remark was the low EEG amplitude that was already observed at the start of EEG monitoring in three SHAM animals. This could be caused by the inoculation of GB cells in the entorhinal cortex (part of the hippocampus) and EEG registration in the same hippocampus. This hypothesis can be tested in a future experiment where baseline EEG will be recorded before the inoculation of the F98 cells. Secondly, the animals were only observed until day 14 which forms the most plausible reason together with the administration of Baytril® and Metacam® in VNS rat 2 why only one out of six animals had epileptic seizures. A previous EEG monitoring study in this GB-related epilepsy rat model concluded that out of seven animals, four animals presented with seizures before post-inoculation day 14. Two out of these four animals presented with only one seizure by this time[33]. Moreover, before day 15 all seven animals presented with seizures and only three out of the seven animals had more than one seizure by then. In addition, progressively

more seizures were observed after day 14 in this previous study[33]. Since the animals of this study were only monitored until day 14 and two animals had missing EEG data of the last day, seizures could have been missed in the animals. In conclusion, longer EEG monitoring of the animals in future studies will reveal more seizures provoked by GB. Therefore, it should be considered to perfuse the animals later than day 14 but before human endpoints are reached (usually day 21 post-inoculation in this model)[33].

Tumour volume

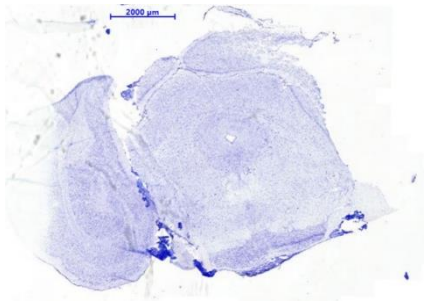

Figure 24. A failed brain slice of VNS rat 3 where clearly part of the tumour is missing (tumour is located at the right of the picture).

It cannot be concluded from this study whether VNS has an effect on GB progression. The reason for this is the lack of data on tumour volumes in 50% of the animals (n=3) due to the bad slices and missing parts of the tumour on the slices (Figure 24), resulting in a low sample size. In VNS rat 3 problems during the perfusion could explain the bad slices. The tumour partly fell out when the brain was isolated. For the other two animals, no reasonable explanation can be found. Fatigue could have played a role while these sections were made. It has been noticed that all animals reacted heavily when applying the ice cold PBS during the perfusion. This never happened before and could have influenced the slicing. In literature, paraffin embedded coupes are usually used to analyse gliomas in rodent models[59]. Therefore, bad slices can be possibly avoided by using PBS (room temperature) followed by 4% PFA instead off saline (room temperature) followed by ice cold PBS during transcardial perfusion and then store the isolated brains in 4% PFA for 24 hours, followed by dehydration steps and paraffin embedding[59]. In the end, one SHAM animal (SHAM rat 1) and two VNS animals (VNS rat 1 and 2) had good consecutive slices from which representative tumour volumes could be calculated. Since the mean tumour volume in the VNS animals (9.92 ± 2.46mm^3) was smaller than the tumour volume in the SHAM animal (16.96mm^3), VNS had a potential negative effect on GB progression which could not be confirmed statistically. Further research and data collection is necessary.

Conclusion

The potential inhibiting effect of VNS on GB progression and seizure frequency in a GB-related epilepsy rat model could not be confirmed based on the results obtained in this master thesis. The tumour volumes of two VNS animals (VNS rat 1 and 2) were relatively smaller than the tumour volume of a SHAM animal (SHAM rat 1) which could not be statistically confirmed. However, this observation can possibly reject arguments saying that VNS can enhance glioma progression by the release of extra GABA[15,29]. Furthermore, the effect of VNS on GB-related seizures could not be observed as the EEG monitoring was too short to record seizures in all (SHAM) animals. This feasibility study revealed important issues (e.g. longer EEG monitoring, perfusion method, paraffin embedding) to be adapted in future experiments. By adapting these procedures future research on bigger sample sizes will be more conclusive to investigate the effect of VNS on GB progression and related seizures.

2. Low-grade glioma rodent model

Immunocytochemistry

The obtained results from the immunocytochemistry staining of the grade I and II cells can be questioned since the GFAP expression patterns differed from the observations in literature. In most studies, higher GFAP expression patterns are observed in LGGs compared to grade IV gliomas and therefore a higher GFAP expression pattern in the grade I and II cells was expected[44]. Furthermore, grade I and II cells have an astrocytic origin resulting in GFAP expression. However, after two immunocytochemistry stainings with GFAP, the cells did not

show expression patterns for GFAP. The lack of GFAP expression observed in these cell lines can be explained by many factors. There can be a loss of astroglial markers and the phenotype of glioma cells when these cells were cultured *in vitro* for several passages[60,61]. GFAP positive human glioma cells of all grades lost their GFAP expression patterns after the 5th or 6th passage[62]. Moreover, cell culture conditions can selectively favour the cells which are dividing more rapidly and are less differentiated. Since less differentiated astrocytes are characterised by lower GFAP expression, this can be a plausible explanation of the negative GFAP expression patterns in the LGG cell lines[62]. In literature, the expression of GFAP in the LGG cell lines is described without mentioning the number of passages before analysis[63]. Therefore, the extra passages *in vitro* of these human LGG cell lines could lead to their negative GFAP expression patterns.

Another reason for the negative GFAP expression patterns could be the epigenetic silencing of the *GFAP* promotor gene[51]. Hypermethylation of the *GFAP* gene is observed in GFAP-negative human glioma cell lines. Hypermethylation of a gene promotor or a gene itself is responsible for the inhibition of gene expression, thereby GFAP will not be expressed when the gene itself or the promotor is methylated. Since GFAP expression of the grade I and II cell line is observed in previous studies, the epigenetic silencing of the GFAP gene should have been changed over time when the cell cultures were passed for several times[49]. In literature, it is stated that the epigenetic regulation of genes in glioma cells can evolve in culture depending on their environmental conditions[53]. Selective pressure of the environmental conditions could be one possible explanation for the epigenetic adaptations of the cell lines. Therefore, long-time cell culturing of the LGG cell lines can possibly result in a methylated *GFAP* promotor. Further research is needed to confirm this hypothesis. As stated before, changes in gene expression over time, culture conditions and methodological differences between research groups are also considered in literature to explain the weak GFAP expression pattern of the grade II cell line[49]. Therefore, they are considered as the most plausible reasons for the negative GFAP expression patterns of the human LGG cell lines. Furthermore, other GFAP antibody concentrations (1:50 vs. 1:1000 in our study) were used in studies showing GFAP expression in grade I cells and a weak expression in grade II cells. Thereby the lower antibody concentration in our study can also be a reasonable explanation for the negative GFAP expression patterns. In addition, rat glioma cells (F98 cells) do not lose their GFAP expression patterns after several passages *in vitro* and the F98 cells stained positive for GFAP during the immunocytochemistry staining[65]. The most plausible explanation for the loss of GFAP expression in the human glioma cell lines is therefore the epigenetic silencing caused by several passages *in vitro.* Literature stated that there was bright GFAP expression in the grade I and II cells after respectively 100 and 50 passages[41]. Factors influencing GFAP expression such as epigenetic silencing caused by several passages could be questioned. Further research is crucial to conclude whether or not these cells express GFAP after several passages *in vitro*.

The expression patterns of vimentin and nestin in the grade I and II cell lines were as expected. First, nestin expression was weakly observed in the grade II cells and none in the grade I cells. Moreover, the same expression patterns were observed in literature[49]. Secondly, vimentin expression patterns observed in the grade I and II cells were similar to the ones described in literature[63]. Since vimentin can be used as an astrocytic marker the expression of vimentin in the grade I and II cell lines confirmed their astrocytic origin[45]. Additionally, the potential of nestin to function as an HGG marker as suggested in literature, was confirmed in this study[47]. The expression of nestin was higher in the F98 cells than compared to the LGG cell lines where the grade II cell line expressed more nestin than grade I cell line. Furthermore, the expected higher vimentin expression in the F98 cells could not be confirmed in this study due to the lack of data caused by the Sars-CoV-2 pandemic[45]. Nevertheless, vimentin expression was observed *in vivo* in the F98 GB tumours[33].

Concluding, the GFAP expression patterns of the grade I and II cell lines differ from the expression patterns observed in literature. Further research to study epigenetic silencing of the *GFAP* promotor and the loss of GFAP expression after several passages is needed. The astrocytic origin of these cell lines (grade I and II) was confirmed by their positive vimentin expression patterns[45]. No evolution towards HGG was observed *in vitro* as the cell lines had a stable doubling time over several passages and no or little nestin expression was observed in the grade I and II cell lines respectively[47].

In vivo low-grade glioma model

In general, no tumour growth was observed in the three non-immunocompromised rats. This can be explained by the human origin of the grade I and II cell lines, the little amount of cells that were injected, the place of injection for the grade I cell line and the short time frame during which the animals were observed. Since the immune system of non-immunodeficient rats can react against the human characteristics of these cell lines, the cells could be rejected by the rats' immune system and as a result the tumour would not grow. Therefore, immunocompromised rodents are usually used to establish glioma models based on gliomas of human origin[66]. Thereby, the obtained results in the non-immunocompromised animals were not surprising. Nonetheless, these experiments were conducted as glioma models which are conducted in immunocompromised animals having a reduced intratumoral heterogeneity and lacking an inherent immune system[66]. Genetic, epigenetic and intratumoral heterogeneity similarity together with an adequate microenvironment are key requirements of a glioma model. As these requirements are not guaranteed, a glioma model in immunocompromised animals is less desired than in normal rats.

Since no tumour growth was observed in the non-immunocompromised rats, a T cell deficient RNu rat was used. In this rat the inoculation of 20 000 grade I and 20 000 grade II cells was insufficient to evoke any tumour growth after 66 days. Therefore, the RNu rat would be inoculated with 100 000 grade II cells at each side after a last T2 scan confirming no tumour growth. This surgery was not feasible due to the Sars-CoV-2 pandemic. In addition, an *ex vivo* T2 MRI would be made of the perfused brain (day 109 post inoculation) to definitely exclude tumour growth, but also this result is not available due to the Sars-CoV-2 pandemic.

Conclusion

LGGs can be symptomatically distinguished from HGGs by their higher seizure frequency and longer overall survival[2,8]. Therefore, an LGG-related epilepsy rodent model is crucial for the investigation of candidate treatments for glioma-related epilepsy, like VNS. As seizures are a more prevalent symptom in diffuse astrocytomas (grade II cell line) than in PA (grade I cell line), the cell line used for the establishment of an LGG-related epilepsy rodent model should be reconsidered[40,42]. Only the grade II cell line should be used in further research.

For further experiments towards an LGG model, a first good step would be the development of an LGG model in an immunocompromised rat. As previous immunocompromised glioma models have provided reproducible tumours[55]. Since the obtained results from the immunocytochemistry staining of the grade II cells suggest epigenetic, genetic or phenotypic changing after several passages in culture, this should be investigated first. This is possible because a part of the cells were frozen after two passages. If this study points out that the characteristics of these cells did change after several passages in culture, a patient derived orthotopic xenograft can be used[66]. Otherwise, the cells can be used after several passages and 100 000 grade II cells in 5µl PBS should be injected into the entorhinal cortex of an immunocompromised rat. After the establishment of an immunocompromised LGG model a next step is the transformation of this model towards a non-immunocompromised animal. In an immunocompromised model the lack of an inherent immune system and TME will result in not presentative reactions towards potential therapeutics and will not allow the role of immune surveillance escape in tumour development[66,67]. To avoid the graft vs. host reaction against

the human origin of the injected tumour cells, a humanised rat can be used[66]. Since humanised rats are very expensive, an alternative where T cell activation is transiently blocked during the inoculation phase could be used[68]. This technique led to the successful engraftment of human tumour cells in immunocompetent mice without further adaptations to the immune system.

In conclusion, the characteristics of the grade II cell line after several passages *in vitro* should be investigated before proceeding to the next steps in developing an LGG-related epilepsy rodent model. It is important for LGG patients and society that the search for a diffuse astrocytoma- or other LGG-related epilepsy rodent models is not stopped due to the its huge challenges. The observations of this master thesis have to be taken into account for the future research.

REFERENCES

1. Ostrom, Q. T. *et al.* The epidemiology of glioma in adults: a 'state of the science' review. *Neuro-Oncology* **16**, 896–913 (2014).

2. Stupp, R. *et al.* High-grade glioma: ESMO Clinical Practice Guidelines for diagnosis, treatment and follow-up. *Annals of Oncology* **25**, iii93–iii101 (2014).

3. Blackburn, D., Sargsyan, S., Monk, P. N. & Shaw, P. J. Astrocyte function and role in motor neuron disease: A future therapeutic target? *Glia* **57**, 1251–1264 (2009).

4. Butt, A. M. Oligodendrocyte Morphology. in *Encyclopedia of Neuroscience* 203–208 (Elsevier, 2009). doi:10.1016/B978-008045046-9.01017-2.

5. Wolburg, H., Wolburg-Buchholz, K., Mack, A. F. & Reichenbach, A. Ependymal Cells. in *Encyclopedia of Neuroscience* 1133–1140 (Elsevier, 2009). doi:10.1016/B978-008045046-9.01001-9.

6. Augusto-Oliveira, M. *et al.* What Do Microglia Really Do in Healthy Adult Brain? *Cells* **8**, 1293 (2019).

7. Chen, R., Smith-Cohn, M., Cohen, A. L. & Colman, H. Glioma Subclassifications and Their Clinical Significance. *Neurotherapeutics* **14**, 284–297 (2017).

8. Huang, C. *et al.* Predictors and mechanisms of epilepsy occurrence in cerebral gliomas: What to look for in clinicopathology. *Experimental and Molecular Pathology* **102**, 115–122 (2017).

9. Stupp, R., Tonn, J.-C., Brada, M., Pentheroudakis, G. & On behalf of the ESMO Guidelines Working Group. High-grade malignant glioma: ESMO Clinical Practice Guidelines for diagnosis, treatment and follow-up. *Annals of Oncology* **21**, v190–v193 (2010).

10. Bell, E. H. *et al.* Association of *MGMT* Promoter Methylation Status With Survival Outcomes in Patients With High-Risk Glioma Treated With Radiotherapy and Temozolomide: An Analysis From the NRG Oncology/RTOG 0424 Trial. *JAMA Oncol* **4**, 1405 (2018).

11. Jenkins, R. B. *et al.* A t(1;19)(q10;p10) Mediates the Combined Deletions of 1p and 19q and Predicts a Better Prognosis of Patients with Oligodendroglioma. *Cancer Res* **66**, 9852–9861 (2006).

12. Maschio, M. Brain Tumor-Related Epilepsy. *CN* **10**, 124–133 (2012).

13. Fisher, R. S. *et al.* Epileptic Seizures and Epilepsy: Definitions Proposed by the International League Against Epilepsy (ILAE) and the International Bureau for Epilepsy (IBE). *Epilepsia* **46**, 470–472 (2005).

14. Englot, D. J., Chang, E. F. & Vecht, C. J. Epilepsy and brain tumors. *Handb Clin Neurol* **134**, 267–285 (2016).

15. Pallud, J., Capelle, L. & Huberfeld, G. Tumoral epileptogenicity: How does it happen? *Epilepsia* **54**, 30–34 (2013).

16. Lewerenz, J. *et al.* The Cystine/Glutamate Antiporter System x_c^- in Health and Disease: From Molecular Mechanisms to Novel Therapeutic Opportunities. *Antioxidants & Redox Signaling* **18**, 522–555 (2013).

17. Salim, S. Oxidative Stress and the Central Nervous System. *J Pharmacol Exp Ther* **360**, 201–205 (2017).

18. Albrecht, P. *et al.* Mechanisms of Oxidative Glutamate Toxicity: The Glutamate/Cystine Antiporter System xc¯ as a Neuroprotective Drug Target. *CNSNDDT* **9**, 373–382 (2010).

19. Moore, Y. E., Kelley, M. R., Brandon, N. J., Deeb, T. Z. & Moss, S. J. Seizing Control of KCC2: A New Therapeutic Target for Epilepsy. *Trends in Neurosciences* **40**, 555–571 (2017).

20. Habela, C. W. & Sontheimer, H. Cytoplasmic Volume Condensation Is an Integral Part of Mitosis. *Cell Cycle* **6**, 1613–1620 (2007).

21. Reijmen, E., Vannucci, L., De Couck, M., De Grève, J. & Gidron, Y. Therapeutic potential of the vagus nerve in cancer. *Immunology Letters* **202**, 38–43 (2018).

22. Hambardzumyan, D., Gutmann, D. H. & Kettenmann, H. The role of microglia and macrophages in glioma maintenance and progression. *Nat Neurosci* **19**, 20–27 (2016).

23. Allavena, P., Sica, A., Solinas, G., Porta, C. & Mantovani, A. The inflammatory micro-environment in tumor progression: The role of tumor-associated macrophages. *Critical Reviews in Oncology/Hematology* **66**, 1–9 (2008).

24. *Glioblastoma*. (Codon Publications, 2017). doi:10.15586/codon.glioblastoma.2017.

25. Oberheim Bush, N. A. & Chang, S. Treatment Strategies for Low-Grade Glioma in Adults. *JOP* **12**, 1235–1241 (2016).

26. Vecht, C. J. & Wilms, E. B. Seizures in low- and high-grade gliomas: current management and future outlook. *Expert Review of Anticancer Therapy* **10**, 663–669 (2010).

27. Vecht, C. *et al.* Seizure response to perampanel in drug-resistant epilepsy with gliomas: early observations. *J Neurooncol* **133**, 603–607 (2017).

28. Vonck, K. *et al.* The Mechanism of Action of Vagus Nerve Stimulation for Refractory Epilepsy: The Current Status. *Journal of Clinical Neurophysiology* **18**, 394–401 (2001).

29. Pérez-Carbonell, L., Faulkner, H., Higgins, S., Koutroumanidis, M. & Leschziner, G. Vagus nerve stimulation for drug-resistant epilepsy. *Pract Neurol* practneurol-2019-002210 (2019) doi:10.1136/practneurol-2019-002210.

30. Vonck, K. *et al.* Vagus nerve stimulation…25 years later! What do we know about the effects on cognition? *Neuroscience & Biobehavioral Reviews* **45**, 63–71 (2014).

31. Pavlov, V. A., Wang, H., Czura, C. J., Friedman, S. G. & Tracey, K. J. The cholinergic anti-inflammatory pathway: a missing link in neuroimmunomodulation. *Mol. Med.* **9**, 125–134 (2003).

32. Zhou, L. *et al.* Neuroprotective effects of vagus nerve stimulation on traumatic brain injury. *Neural Regen Res* **9**, 1585–1591 (2014).

33. Bouckaert, C. *et al.* Development of a rat model for glioma-related epilepsy. Manuscript in preparation.

34. Jadus, M. *et al.* Mechanisms of immune evasion exhibited by different rat glioma cell lines. in *Neuro-Oncology and Cancer Targeted Therapy* 109–139 (2010).

35. Hambardzumyan, D., Gutmann, D. H. & Kettenmann, H. The role of microglia and macrophages in glioma maintenance and progression. *Nat Neurosci* **19**, 20–27 (2016).

36. Boon, P., De Cock, E., Mertens, A. & Trinka, E. Neurostimulation for drug-resistant epilepsy: a systematic review of clinical evidence for efficacy, safety, contraindications and predictors for response. *Current Opinion in Neurology* **31**, 198–210 (2018).

37. Hu, X. & Holland, E. C. Applications of mouse glioma models in preclinical trials. *Mutation Research/Fundamental and Molecular Mechanisms of Mutagenesis* **576**, 54–65 (2005).

38. Chen, Y.-H. *et al.* Mouse Low-Grade Gliomas Contain Cancer Stem Cells with Unique Molecular and Functional Properties. *Cell Reports* **10**, 1899–1912 (2015).

39. Sievert, A. J. & Fisher, M. J. Pediatric Low-Grade Gliomas. *J Child Neurol* **24**, 1397–1408 (2009).

40. Collins, V. P., Jones, D. T. W. & Giannini, C. Pilocytic astrocytoma: pathology, molecular mechanisms and markers. *Acta Neuropathol* **129**, 775–788 (2015).

41. Bobola, M. S. O6-Methylguanine-DNA Methyltransferase, O6-Benzylguanine, and Resistance to Clinical Alkylators in Pediatric Primary Brain Tumor Cell Lines. *Clinical Cancer Research* **11**, 2747–2755 (2005).

42. Lind-Landström, T., Habberstad, A. H., Sundstrøm, S. & Torp, S. H. Prognostic value of histological features in diffuse astrocytomas WHO grade II. *Int J Clin Exp Pathol* **5**, 152–158 (2012).

43. McKeon, A. & Benarroch, E. E. Glial fibrillary acid protein: Functions and involvement in disease. *Neurology* **90**, 925–930 (2018).

44. Sereika, M., Urbanaviciute, R., Tamasauskas, A., Skiriute, D. & Vaitkiene, P. *GFAP* expression is influenced by astrocytoma grade and *rs2070935* polymorphism. *J. Cancer* **9**, 4496–4502 (2018).

45. Lin, L. *et al.* Analysis of expression and prognostic significance of vimentin and the response to temozolomide in glioma patients. *Tumor Biol.* **37**, 15333–15339 (2016).

46. Schnitzer, J., Franke, W. & Schachner, M. Immunocytochemical demonstration of vimentin in astrocytes and ependymal cells of developing and adult mouse nervous system. *The Journal of Cell Biology* **90**, 435–447 (1981).

47. Zhang, M. *et al.* Nestin and CD133: valuable stem cell-specific markers for determining clinical outcome of glioma patients. *J Exp Clin Cancer Res* **27**, 85 (2008).

48. Johnson, M. Fetal Bovine Serum. *MATER METHODS* **2**, (2012).

49. El Tahry, R. *et al.* Repeated assessment of larynx compound muscle action potentials using a self-sizing cuff electrode around the vagus nerve in experimental rats. *Journal of Neuroscience Methods* **198**, 287–293 (2011).

50. Van Lysebettens, W. *et al.* Hypothermia Masks Most of the Effects of Rapid Cycling VNS on Rat Hippocampal Electrophysiology. *Int. J. Neur. Syst.* **29**, 1950008 (2019).

51. Lysebettens, W. V. *et al.* TEMPERATURE-INDEPENDENT EFFECTS OF VAGUS NERVE STIMULATION ON RAT HIPPOCAMPAL ELECTROPHYSIOLOGY. Manuscript in preparation.

52. Albulescu, R. *et al.* Cytokine Patterns in Brain Tumour Progression. *Mediators of Inflammation* **2013**, 1–7 (2013).

53. Li, G. *et al.* Cytokines and epilepsy. *Seizure* **20**, 249–256 (2011).

54. Lehtimäki, K. A. *et al.* Regulation of IL-6 system in cerebrospinal fluid and serum compartments by seizures: the effect of seizure type and duration. *Journal of Neuroimmunology* **152**, 121–125 (2004).

55. Dai, C. & Holland, E. C. Glioma models. *Biochimica et Biophysica Acta (BBA) - Reviews on Cancer* **1551**, M19–M27 (2001).

56. Mitsuhashi, S. *et al.* Fluorinated quinolones — new quinolone antimicrobials. in *Progress in Drug Research / Fortschritte der Arzneimittelforschung / Progrès des recherches pharmaceutiques* (ed. Jucker, E.) 9–147 (Birkhäuser Basel, 1992). doi:10.1007/978-3-0348-7141-9_1.

57. Lee, J. W. *et al.* Morphological Characteristics of Brain Tumors Causing Seizures. *Arch Neurol* **67**, (2010).

58. Henker, C. *et al.* Association Between Tumor Compartment Volumes, the Incidence of Pretreatment Seizures, and Statin-Mediated Protective Effects in Glioblastoma. *Neurosurgery* **85**, E722–E729 (2019).

59. Garcia, C. *et al.* The orthotopic xenotransplant of human glioblastoma successfully recapitulates glioblastoma-microenvironment interactions in a non-immunosuppressed mouse model. *BMC Cancer* **14**, 923 (2014).

60. Knott, J. C., Edwards, A. J., Gullan, R. W., Clarke, T. M. & Pilkington, G. J. A human glioma cell line retaining expression of GFAP and gangliosides, recognized by A2B5 and LB1 antibodies, after prolonged passage. *Neuropathol. Appl. Neurobiol.* **16**, 489–500 (1990).

61. Restrepo, A. *et al.* Epigenetic regulation of glial fibrillary acidic protein by DNA methylation in human malignant gliomas. *Neuro-Oncology* **13**, 42–50 (2011).

62. Lolait, S. J., Harmer, J. H., Auteri, G., Pedersen, J. S. & Toh, B. H. Expression of glial fibrillary acidic protein, actin, fibronectin and factor VIII antigen in human astrocytomas. *Pathology* **15**, 373–378 (1983).

63. Bax, D. A. *et al.* Molecular and Phenotypic Characterisation of Paediatric Glioma Cell Lines as Models for Preclinical Drug Development. *PLoS ONE* **4**, e5209 (2009).

64. Baysan, M. *et al.* Micro-Environment Causes Reversible Changes in DNA Methylation and mRNA Expression Profiles in Patient-Derived Glioma Stem Cells. *PLoS ONE* **9**, e94045 (2014).

65. Reifenberger, G., Bilzer, T., Seitz, R. J. & Wechsler, W. Expression of vimentin and glial fibrillary acidic protein in ethylnitrosourea-induced rat gliomas and glioma cell lines. *Acta Neuropathol* **78**, 270–282 (1989).

66. Lenting, K., Verhaak, R., ter Laan, M., Wesseling, P. & Leenders, W. Glioma: experimental models and reality. *Acta Neuropathol* **133**, 263–282 (2017).

67. Guerrero-Cázares, H., Chen, L. & Quiñones-Hinojosa, A. Glioblastoma Heterogeneity and More Accurate Representation in Research Models. *World Neurosurgery* **78**, 594–596 (2012).

68. Semenkow, S. *et al.* An immunocompetent mouse model of human glioblastoma. *Oncotarget* **8**, 61072–61082 (2017).

In vitro and in vivo evaluation of Low-Grade Glioma

Delphine Dhont [1], Charlotte Bouckaert [1], Kristl Vonck [1], Robrecht Raedt [1]

[1] 4BRAIN lab,
Department of Head and Skin, Ghent University, Belgium.

Corresponding author: Delphine.Dhont@UGent.be

Introduction

- Gliomas represent 81% of primary intracranial malignant brain tumours
- Epileptic seizures are the most common symptom in patients with glioma
- Prevalence of epileptic seizures in low-grade glioma is 50-90% and in high-grade glioma 20-60%
- Approximately 30% of glioma patients develop refractory epilepsy
- Standard treatment for low-grade glioma has adverse effects on the quality of life of the patient
- Preclinical model for low-grade glioma is desired for research on alternative treatments targetting tumour growth and seizure frequency

Methods

Cell culture

1. Res186: Human pilocytic astrocytoma grade I
2. Res259: Human diffuse astrocytoma grade II

→ DMEM/F12 Ham's medium

1. Characterization of glioma cells

Immunocytochemistry staining

Fixation of cells with PFA on coverglass

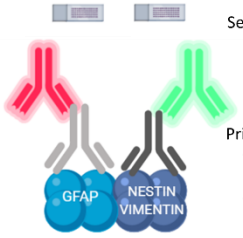

Secondary antibodies:
- Alexa fluor 594 goat anti-rabbit
- Alexa fluor 488 goat anti-mouse

Primary antibodies:
- Polyclonal rabbit anti-GFAP
- Monoclonal mouse anti-vimentin clone V9
- Monoclonal mouse anti-nestin 10c2

2. In vivo low-grade glioma analyses

A. Normal rats

Inoculation → Perfusion on day 14 → Cresyl violet staining → Analyses tumour presence

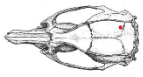

AP: -8,0mm
ML: -4,5mm
DV: -4,1mm

Male Fischer rat (n=1)
20 000 Res259 cells/5µl PBS

Male Sprague Dawley rats (n=2)
20 000 Res259 cells/5µl PBS (n=1)
20 000 Res186 cells/5µl PBS (n=1)

B. T-cell deficient RNu rat

Inoculation

AP: -8,0mm
ML: -4,5mm / +4,5mm
DV: -4,1mm

MRI T2
Day 10, 14, 31, 66

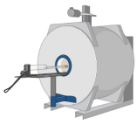

Male RNu rat (n=1)
20 000 Res186 cells/5µl PBS (●)
20 000 Res259 cells/5µl PBS (●)

Results

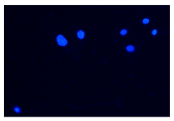

Figure 1. DAPI
Res186 cells

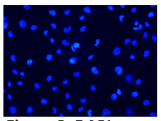

Figure 3. DAPI
Res259 cells

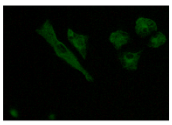

Figure 2. Vimentin
Res186 cells

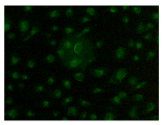

Figure 4. Vimentin
Res259 cells

Figure 5.
20 000 Res259 cells/5µl PBS
No tumour growth observed in normal rats

Figure 6.
20 000 Res186 cells/ 5µl PBS
No tumour growth observed in normal rat

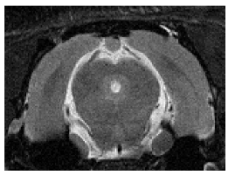

Figure 7. MRI T2 RNu Day 66
No tumour observed

Conclusion

- Cell culture: Expression of Vimentin in both cell lines and no expression profile of GFAP and Nestin
- In vivo: No tumour growth observed in normal rats and RNu rat
- Future perspective RNu rat: Inoculation of 100 000 Res259 cells/5µl PBS left and right (similar coordinates)
  Follow-up of tumour growth with MRI T2

ADDENDUM

1. Cell passage

Cell cultures were split when 80% confluency was achieved. Gloves were always used and regularly disinfected with 70% ethanol. First, the LAF cabinet was put on for 20 minutes and the surface was disinfected using 70% ethanol. The medium, trypsin and phosphate buffered saline (PBS) were put in a hot water bath of 37°C. Once, these substances were warm enough they were disinfected with 70% ethanol and put in the LAF cabinet (disinfection from the bottom to the top).

The cell culture was split as followed:

1. Take off the medium with a pipette of 10ml.
2. Rinse with 5ml PBS. Make sure that the pipette does not touch the cells by holding the falcon in 45° and put the pipette against the bottom (illustrated in figure 25). Once the PBS is in the falcon, put the falcon on the bench and let the PBS run carefully and for a couple of seconds over the cells. Then take off the PBS when holding the T75 falcon in 45° (as illustrated in figure 25).
3. Add 2ml of trypsin to the cells and put the falcon for 5 minutes in the incubator (37°C and 5% CO_2). This step is used to detach the cells from the surface.
4. Add the desired amount of medium to the cells in the trypsin. Remark: for cell counting this is fixed (2ml) for splitting not.
5. Calculate the amount of cell suspension that is needed for the desired dilution of the cell culture and put this in a new T75 falcon. For example, for the F98 cells a dilution of 1/10 is usually used. Therefore, 3ml is of medium is added to the cells in trypsin and 0.5ml is taken of the cell suspension and put in another T75 falcon.
6. Add medium to the new falcon till the falcon contains 10ml in total. And put the T75 falcon again in the incubator.

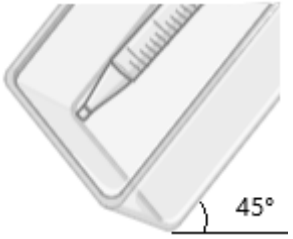

Figure 25. Position of pipette in falcon for rinsing the cell culture with PBS.

2. Low-Grade glioma experiments

2.1 In vivo

2.1.1 Coordinates of inoculation of RNu rat

	Mediolateral	Dorsoventral (dura mater: 0)
Lambda	7.60	/
Res186	7.15	-4.1
Res259	8.05	-4.1

Table 2. Exact coordinates of the RNu rat all coordinates are in mm and measured with the Hamilton needle.

2.1.2 Weight follow-up of the animals

Day post innoculation	Date	Weight of 1st normal animal (g)	Weight of 2nd normal animal (g)	Weight of 3rd normal animal (g)
d0	27/11/2019	350	462	435
d1	28/11/2019	315	445	430
d2	29/11/2019	320	442	425
d3	30/11/2019	320	446	424
d4	1/12/2019	320	444	423
d5	2/12/2019	316	449	428
d6	3/12/2019	323	451	433
d7	4/12/2019	316	453	423
d8	5/12/2019	319	449	430
d9	6/12/2019	317	450	420
d10	7/12/2019	320	453	427
d11	8/12/2019	325	456	437
d12	9/12/2019	328	460	434
d13	10/12/2019	329	468	440
d14	11/12/2019	330	466	437

Table 3. Weight follow-up of the normal animals.

Days post inoculation	Date	Weight of RNu(g)		Days post inoculation	Date	Weight of RNu(g)
day 0	6/12/2019	230		day 28	3/01/2020	289
day 1	7/12/2019	220		day 29	4/01/2020	291
day 2	8/12/2019	222		day 30	5/01/2020	295
day 3	9/12/2019	223		day 31	6/01/2020	301
day 4	10/12/2019	232		day 32	7/01/2020	295
day 5	11/12/2019	233		day 33	8/01/2020	297
day 6	12/12/2019	234		day 34	9/01/2020	302
day 7	13/12/2019	240		day 35	10/01/2020	305
day 8	14/12/2019	245		day 36	11/01/2020	/
day 9	15/12/2019	244		day 37	12/01/2020	/
day 10	16/12/2019	249		day 38	13/01/2020	310
day 11	17/12/2019	247		day 39	14/01/2020	307
day 12	18/12/2019	257		day 40	15/01/2020	309
day 13	19/12/2019	/		day 41	16/01/2020	312
day 14	20/12/2019	260		day 42	17/01/2020	315
day 15	21/12/2019	/		day 43	18/01/2020	317
day 16	22/12/2019	235		day 44	19/01/2020	311
day 17	23/12/2019	271		day 45	20/01/2020	320
day 18	24/12/2019	271		day 46	21/01/2020	324
day 19	25/12/2019	277		day 47	22/01/2020	320
day 20	26/12/2019	276		day 48	23/01/2020	/
day 21	27/12/2019	281		day 49	24/01/2020	/
day 22	28/12/2019	276		day 50	25/01/2020	/
day 23	29/12/2019	279		day 51	26/01/2020	/
day 24	30/12/2019	283		day 52	27/01/2020	330
day 25	31/12/2019	283		day 53	28/01/2020	/
day 26	1/01/2020	289		day 54	29/01/2020	331
day 27	2/01/2020	294				

Table 4. Weight follow-up of RNu rat.

3. Tumour volumes

3.1 VNS rat 1

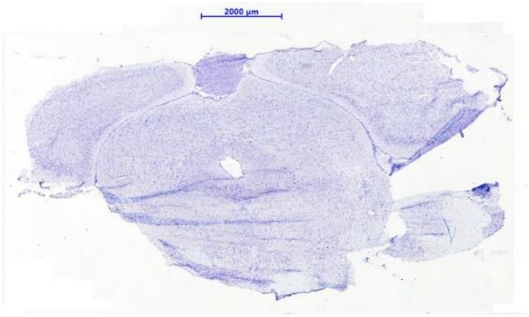

(10)

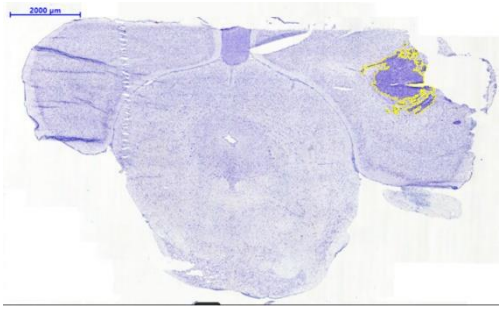

(11)

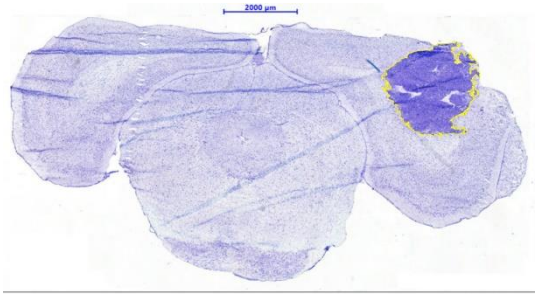

(12)

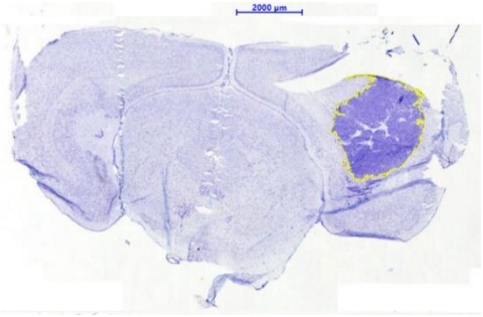

(13)

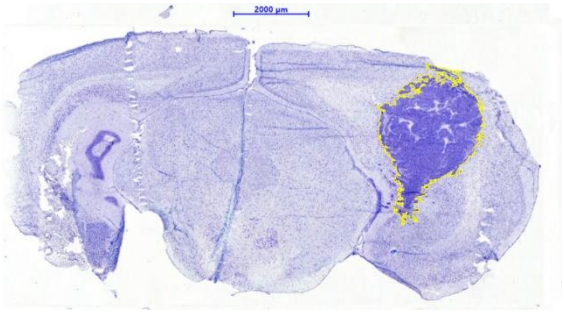

(14)

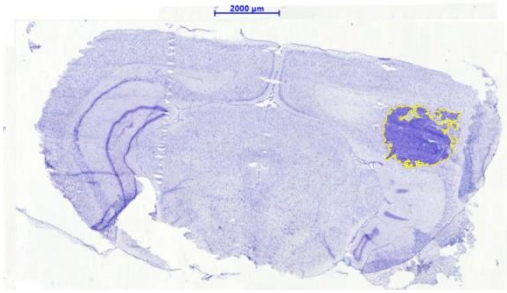

(15)

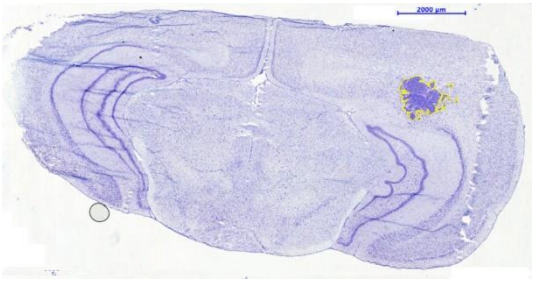

(16)

Slice n°	area (mm²)	volume (mm³) = area * 0,5
10	part of tumour gone?	
11	1,782	0,891
12	4,614	2,307
13	6,174	3,087
14	6,558	3,279
15	3,098	1,549
16	1,089	0,5445
total volume in (mm³)		11,6575
total amount of cells injected		20 122,125

Figure 26. This figure illustrates the slices representing tumour and the volume calculations of VNS rat 1.

3.2 SHAM rat 1

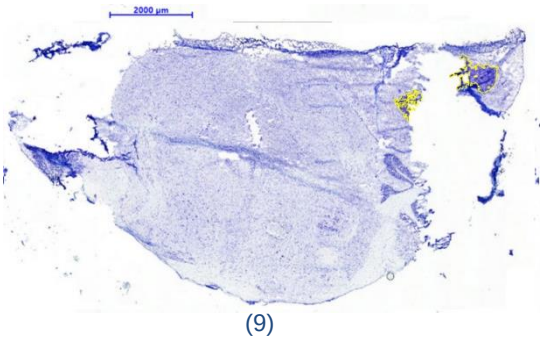

(9)

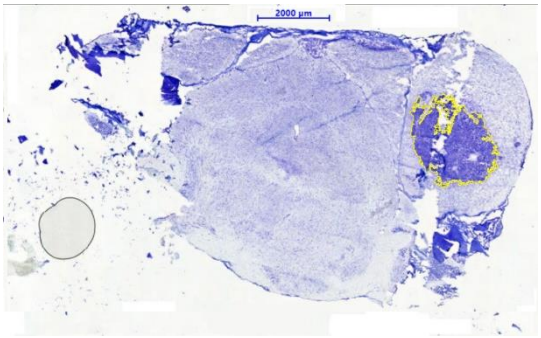

(10)

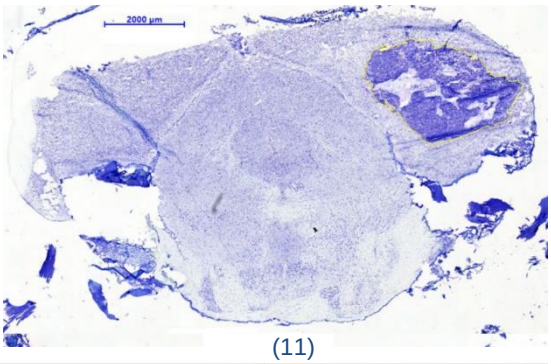

(11)

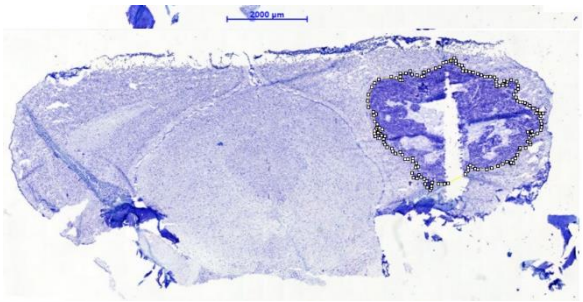

(12)

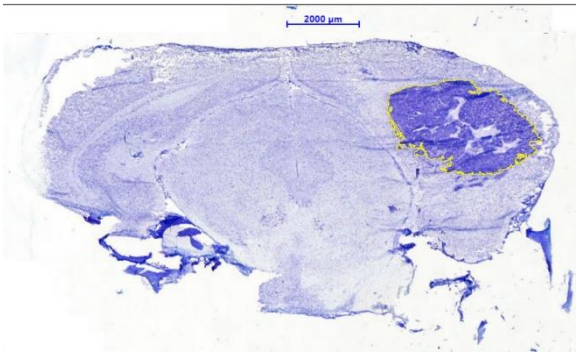

(13)

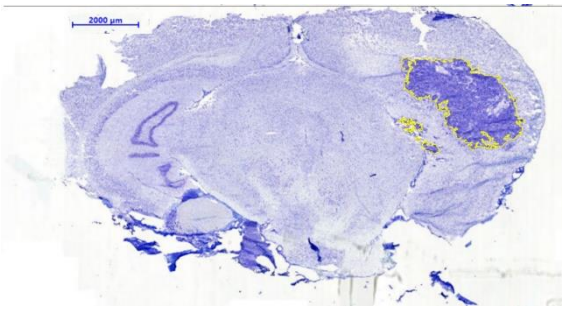

(14)

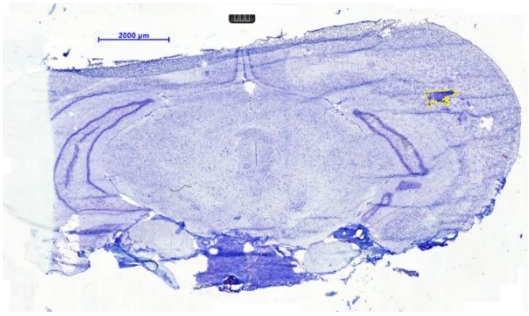

(15)

Slice n°	area (mm^2)	volume (mm^3) = area*0,5
9	0,599	0,2995
10	3,968	1,984
11	6,604	3,302
12	8,902	4,451
13	7,55	3,775
14	6,058	3,029
15	0,234	0,117
total volume (mm^3)		16,9575
total amount of cells injected		20 842

Figure 27. This figure illustrates the slices representing tumour and the volume calculations of SHAM rat 1.

3.3 VNS rat 2

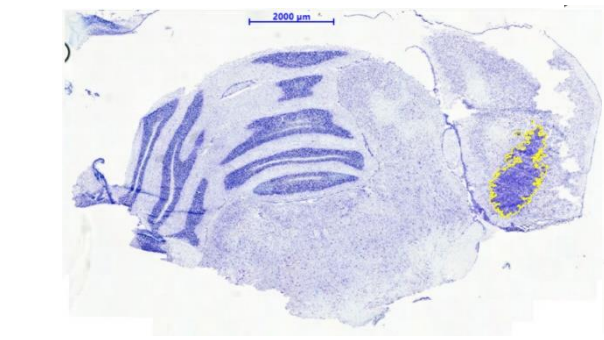

(6)

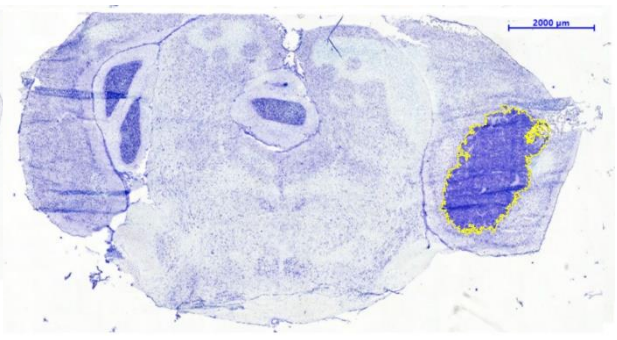

(7)

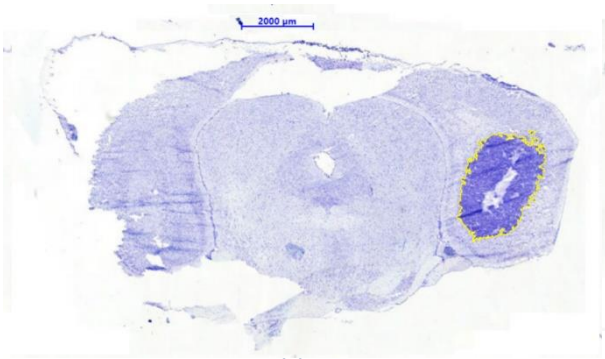

(8)

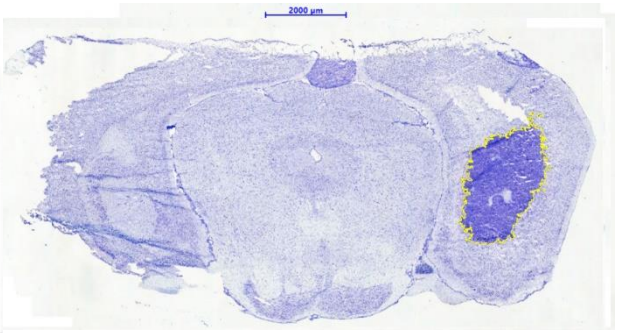

(9)

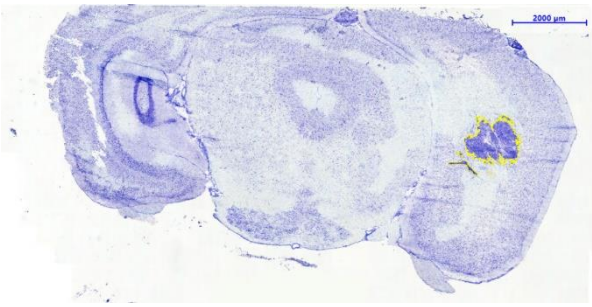

(10)

Slice n°	area (mm²)	volume (mm³) =area*0,5
6	1,461	0,7305
7	4,387	2,1935
8	4,864	2,432
9	4,304	2,152
10	1,349	0,6745
total volume (mm³)		8,1825
total amount of cells injected		20 106

Figure 28. This figure illustrates the slices representing tumour and the volume calculations of VNS rat 2.

3.4 Tumour volumes of all animals

Animal	Tumour volume (mm^3)	Total amount of cells injected
died	/	11 000
1st VNS	11.66	20 122
died	/	20 800
1st SHAM	16.96	20 842
2nd VNS	8.18	20 106
3rd VNS	10.92	20 720
2nd SHAM	9.70	20 222
3rd SHAM	8.03	20 826

Table 5. Calculated tumour volumes of all animals and the total amount of cells injected. The 3rd VNS, 2nd and 3rd SHAM animals were excluded for analyses because these slices were not reliable.

4. T2*-weighted MRI RNu

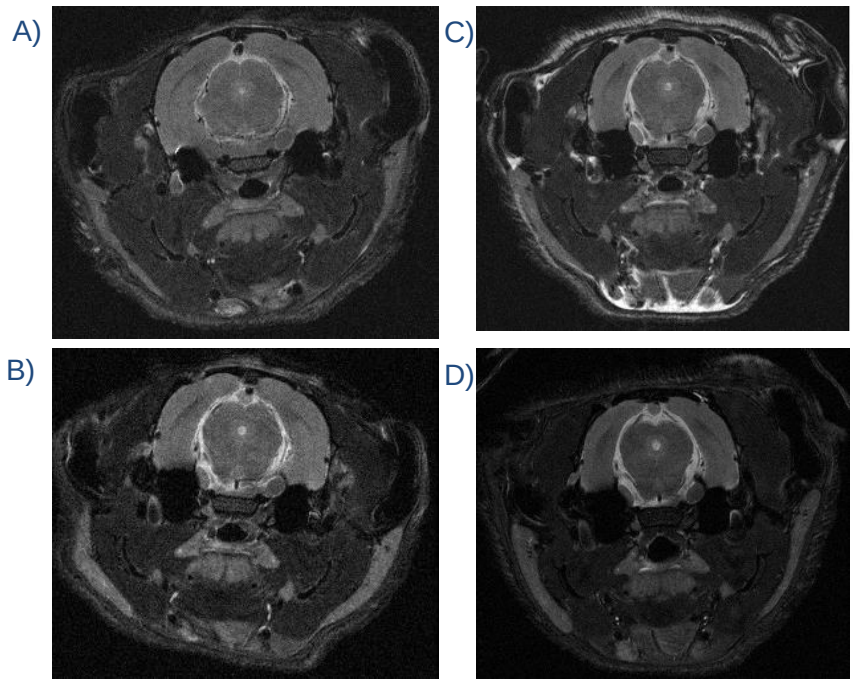

Figure 29. T2 MRI scans of the RNu rat at the inoculation site. A) ilustrates the MRI taken at day 10, B) day 14, C) day 31 and D) day 61.

5. Abbreviations

ABC	ATP-binding cassette
Ach	acetylcholine
ACTH	adrenocorticotrophic hormone
AEDs	anti-epileptic drugs
α7nAchR	α seven subunit nicotinic acetylcholine receptor
ATP	adenosine triphosphate
BBB	blood-brain barrier
BDNF	brain-derived neurotrophic factor
CNS	central nervous system
CRP	corticotrophin releasing hormone
CSF	cerebrospinal fluid
CYP	cytochrome P450
DMEM	Dulbecco's Modified Eagle Medium
EAATs	excitatory amino acid transporters
EEG	electroencephalography
EMT	epithelial to mesenchymal transition
FCS	fetal calf serum
GABBA	gamma-aminobutyric acid
GB	glioblastoma
GFAP	glial filament acidic protein
Glu	glutamate
GSH	glutathione
HGGs	high-grade gliomas
HPA	hypothalamic-pituitary-adrenal
IDH	isocitrate dehydrogenase
IL-1	interleukin 1
IL-10	interleukin 10
IL-13	interleukin 13
IL-18	interleukin 18
IL-1β	interleukin 1β
IL-4	interleukin 4
IL-6	interleukin 6
ILAE	International League Against Epilepsy
KCC2	potassium chloride co-transporter
LC	locus coeruleus
LGGs	low-grade gliomas
LOH	loss of heterozygosity
MDR-1	P-glycoprotein
MGMT	methyl-guanine methyl transferase
MRI	magnetic resonance imaging
NF-κB	nuclear factor κB
NKCC1	$Na^+/K^+/2Cl^-$ co-transporter 1
NSAID	non-steroidal anti-inflammatory drugs
NT	neurotransmitter
NTS	nucleus tractus solitarii

PA	pilocytic astrocytoma
PBS	phosphate buffered saline
PFA	paraformaldehyde
PVN	paraventricular nucleus
ROS	reactive oxygen species
RT	radiotherapy
RVM	rostral ventrolateral medulla
TAMs	tumour associated macrophages
TME	tumour microenvironment
TMZ	temozolomide
TNF-α	tumour necrosis factor α
UGT	UDP-glucuronosyltransferase
VNS	vagus nerve stimulation
WHO	World Health Organisation